OPTIMIZATION OF PROCESS PARAMETERS IN LASER WELDING OF DISSIMILAR MATERIALS IN LAP JOINT CONFIGURATION USING MULTI-OBJECTIVE TAGUCHI ANALYSIS

A THESIS SUBMITTED IN PARTIAL FULFILLMENT
OF THE REQUIREMENT FOR THE DEGREE OF

MASTER OF TECHNOLOGY

In

Mechanical Engineering

By

ASIT BEHERA
Roll No: 212ME2292

DEPARTMENT OF MECHANICAL ENGINEERING
NATIONAL INSTITUTE OF TECHNOLOGY
ROURKELA, INDIA
MAY, 2014

OPTIMIZATION OF PROCESS PARAMETERS IN LASER WELDING OF DISSIMILAR MATERIALS IN LAP JOINT CONFIGURATION USING MULTI-OBJECTIVE TAGUCHI ANALYSIS

A THESIS SUBMITTED IN PARTIAL FULFILLMENT OF THE REQUIREMENT FOR THE DEGREE OF

MASTER OF TECHNOLOGY

In

Mechanical Engineering

By

ASIT BEHERA
Roll No: 212ME2292

Under the Guidance of
Prof. S.K. PATEL

DEPARTMENT OF MECHANICAL ENGINEERING
NATIONAL INSTITUTE OF TECHNOLOGY
ROURKELA, INDIA
MAY, 2014

DEDICATED

TO

MY PARENTS AND BROTHER

Declaration

I hereby declare that the work which is being presented in this thesis entitled
"**Optimization of process parameters in laser welding of dissimilar materials in lap joint
configuration using multi-objective Taguchi analysis**" in partial fulfillment of the
requirements for the award of M.Tech. degree, submitted to the Department of Mechanical
Engineering, National Institute of Technology, Rourkela, is an authentic record of my own work
under the supervision of Prof. S.K. Patel. I have not submitted the matter embodied in this thesis
for the award of any other degree or diploma to any other university or Institute.

Date:3-Jun-14   **Asit Behera**

CERTIFICATE

This is to certify that, the thesis entitled "OPTIMIZATION OF PROCESS PARAMETERS IN LASER WELDING OF DISSIMILAR MATERIALS IN LAP JOINT CONFIGURATION USING MULTI-OBJECTIVE TAGUCHI ANALYSIS" being submitted to the National Institute of Technology, Rourkela by Mr. **Asit Behera**, Roll no. 212ME2292 for the award of M.Tech. degree in Mechanical Engineering, is a bona fide record of research work carried out by him under my supervision and guidance.

The candidate has fulfilled all the prescribed requirements. The Thesis which is based on candidate's own work has not been submitted elsewhere for award of any degree. In my opinion, the thesis is of standard required for the award of M.Tech. degree in Mechanical Engineering.

Prof. S.K. Patel
Supervisor
Department of Mechanical Engineering
National Institute of Technology
Rourkela – 769008
Email: skpatel@nitrkl.ac.in

ACKNOWLEDGMENT

<div align="right">

Asit Behera
Roll No: 212ME2292
Mechanical Engineering
NIT Rourkela

</div>

Date:
Place:

CONTENTS

ABSTRACT

The need of joining of dissimilar materials goes on increasing day by day in industry due to its high demand. Dissimilar joints are based on both technical and economical aspects, because they can provide satisfactory service performance and reasonable cost savings. The demand for such joints in industry is huge. For example, in power plant industry more than thousand dissimilar joints are used. Joints between dissimilar metals are particularly common in components used in the automotive, power generation, chemical, petrochemical, nuclear and electronics industries. Dissimilar spot welded joints of medium carbon and stainless steel are currently used for car body assembling. But dissimilar spot welding can be more complicated than similar welding because of different thermo-physical properties of metal and inevitably, various thermal cycle experienced by each metal. So, the study of dissimilar material welding is of a great interest for many of the researchers.

Again, laser welding with high power density, high degree of automation and high production rate is extremely advantageous in industrial applications. Generally when two dissimilar materials are welded by any conventional welding process, then due to inequality in heat conductivity of materials they are not welded properly. But in laser welding as higher energy density is concentrated in small area welding can be done properly irrespective of conductivity of materials. The parameters of laser welding plays important role in determining quality of the weld and hence the quality of the product made in industry. Since the demand of a product depends mostly on its quality, the parameters of laser welding should be optimized properly so as to find good weld quality.

In this project two dissimilar materials namely AISI 316L and AISI 1552 were taken for laser welding in lap joint configuration. Three process parameters i.e. scan speed, pulse frequency and pulse diameter at four levels were taken for optimization. Two response parameters namely weld hardness and length of heat affected zone were considered for different combinations of process parameters. Grey Taguchi methodology with L_{16} orthogonal array was used to optimize specified parameters. It is found that laser welding with scan speed of 45 mm/min, pulse diameter of 0.3 mm and pulse frequency of 7 Hz yields the optimal quality characteristics. In these levels hardness of weld zone was found to be 304.77 HV and length of HAZ to be 0.0852 mm.

LIST OF TABLES

LIST OF FIGURES

CHAPTER 1

INTRODUCTION

1. INTRODUCTION

1.1 OVERVIEW

Laser beam welding is a welding process used to join two metals by the use of a laser source. The laser source provides a concentrated and high density heat source, allowing for narrow, deep weld bead with high welding scan speed. The process is mostly used in high volume production industries, such as in the automotive industry. But now-a-days it has profound application in various metal working fields due to its advantageous effects over other machining operations. Laser beam welding has high power density which results in small heat affected zone due to high heating and cooling rates. Laser beam welding is a versatile process, which can weld almost all materials including aluminum, titanium, carbon steels, HSLA steels and stainless steel.

The laser beam is an efficient technique to join metals. This can join metals at the surface level and also at depth to produce strong welding. It can be associated with conventional welding processes to give required weld quality. The weld quality is high and this can be used for soldering. Materials with high heat conductivity and high melting point such as aluminum can be welded using a laser source with considerable power. Joining and welding of two materials are totally different. Some material can be joined due to the small amount of molten material and the controllable melting period, but could not be welded. Also due to high heating and cooling rates the weld zone is supposed to be micro-cracked.

Laser source is characterized by coherent, collimated source of light. So the supply of energy can be regulated, well monitored and maintained properly in laser welding. Continuous or pulsed laser beam may be used depending upon the various applications in industry. Thin materials are welded by millisecond-long pulses while continuous laser systems are used for deep welds. The laser welding process operates at very high scan speeds with low distortion as intense energy beam of light is used as heat source. Since it requires no filler material, laser welding reduces costs. Laser welding can be automated for a stable, repeatable weld process.

Fig. 1: Laser machine setup

With well-defined beams of high power density, lasers are excellent source for welding thin materials, operating in close proximity to heat-induced components. If a line-of-sight exists even complicated contour portions can be welded by laser. For laser welding the material can be any material which is welded conventionally but the material should be thin. However, lasers can also join materials which are very difficult to weld such as titanium, high carbon stainless steel and aluminum as well as welding dissimilar materials which are mostly incompatible. A schematic picture of laser machine in working condition is shown in Fig. 1.

Laser welding has high power density, large production rate and high degree of automation which makes it extremely advantageous in industrial applications. Joints between dissimilar metals are used in many industrial applications which are particularly common in components used in the automotive, power generation, chemical, petrochemical, nuclear and electronics industries. The ability to use different metals and alloys in a product makes the product more flexible and often results in technical and economic advantages over components produced from a single material. Dissimilar welding now stands as a major scientific and technical challenge for

the engineers. Emerging new technologies with greater flexibility increasingly require dissimilar metals to be joined. Most metals and alloys are weldable in two mechanisms of welding process i.e. either by conduction welding or by keyhole mode welding.

Dissimilar welding are more confused than comparative similar welding as the metals have diverse thermo-physical properties and in particular different unmatched thermal cycle accomplished by each metal. Dissimilar spot welded joints of low carbon and stainless steel are presently utilized for auto body assembly. The need of joining of different materials continues expanding continuously in industry because of its demand. The capacity to utilize distinctive metals within an item gives the design and manufacturing engineer with more adaptability and almost always brings economic and technical advantages over parts produced from a solitary material. Dissimilar welding represents significant exploratory and technical challenge. Developing new innovations like laser beam progressively require dissimilar materials to be joined.

1.2 MOTIVATION

The joints between dissimilar metals are particularly common in components used in the automotive, power generation, chemical, petrochemical, nuclear and electronics industries [1]. The demand for dissimilar joints is much more as they can provide satisfactory service performance at reasonable cost. The demand for such joints in industry is huge. In many cases the use of dissimilar materials increases the whole economy of the system compared to single material. Emerging new technologies increasingly require dissimilar metals and alloys to be joined.

Again, laser welding with high degree of automation, high power density and high production rate is extremely advantageous in industrial applications. The beam provides a concentrated heat source, allowing for narrow and deep welds with high welding rates. The welding technique is repetitively used in high volume applications, such as in the automotive industry. So, optimization of process parameters in laser welding of dissimilar materials is mostly needed for quality improvement.

1.3 OBJECTIVES

The objectives of the thesis are listed below.

❖ To optimise process parameters such as laser scan speed, pulse diameter and pulse frequency by Taguchi analysis

❖ To maximize response i.e. hardness and length of heat affected zone by taking optimized values of input laser parameters

❖ To identify the significant factors using ANOVA

❖ To determine percentage contribution of factors for response

1.4 Thesis organization

Including the introductory chapter, the thesis is divided into 5 chapters. The organization of the thesis is presented below.

Chapter-2: Literature Review

This chapter illustrates the chronological evolution of some techniques in laser welding. Microstructure of weld zone and parameters involved in laser welding are also discussed. It also shows optimization and simulation of process parameters in laser welding of various types of steels at different conditions.

Chapter-3: Experimental Procedure

This chapter describes the detailed procedure of the experiment. This chapter is devoted for all the objectives stated above. It states about different process parameters and responses considered for optimization in welding and also about different machines used at different stages of work. The method of optimization and also the design of experiment are considered in this chapter.

Chapter-4 Results and Discussion

The detailed results found from optimization are presented and discussed in this chapter. The graphs containing main effect plot and residual plot are also presented in this section.

Chapter-5 Conclusions

The overall conclusions of the thesis are presented in this chapter. It also contains some future research areas, which need attention and further investigation.

CHAPTER 2

LITERATURE REVIEW

2.1 LASER

Laser is acronym for the phenomenon called light amplification by simulated emission of radiation. In laser, light amplification takes place through simulated emission of electromagnetic radiation. The phenomenon was first developed by Albert Einstein. However, the first laser was made possible only in 1960 by Maiman [2]. Since then laser has seen various developments.

Laser is special over other source of light because they emit light coherently. This is popularly known as 'pencil beam' as spatial coherence is expressed through the output being a narrow low diameter beam which is diffraction-limited [3]. The application of laser beam in material processing is given in Fig. 2. Temporal or longitudinal coherence describes a polarized wave at a single frequency correlated between value of a wave and itself. Temporal coherence tells us how monochromatic a source is. It characterizes how well a wave can interfere with itself at a defined time. A beam emerged by thermal energy or other incongruous light source generally has a instantaneous amplitude and phase which change arbitrarily concerning time and position. So it has a short coherence length [4].

Fig. 2: Application of Laser beam [5]

The properties of a laser beam that have significant effect on material processing include divergence, coherence, monochromaticity, brightness, stability, size and mode. These are discussed below.

2.1.1 Beam divergence

Beam divergence may be defined as the characteristics of a light beam that results in an increase in its cross-sectional area with increase in distance from source. Light from an ordinary source is distributed uniformly in all directions. So its divergence is considered to be high enough. But in case of laser, the cross-section remains almost constant throughout the path travelled. Hence divergence is very low [6].

The low divergence and thus almost parallel nature of a laser beam facilitates the beam to be focused to a very small radius. The laser source can be concentrated to a diameter of its wavelength. So, large amount of energy is generated at that point. For welding, it is very much necessary to have a highly focused beam. So, a low divergence beam is important for such operation.

2.1.2 Monochromaticity

The monochromatic beam contains only a single wavelength. Lasers are said to be monochromatic because unlike conventional source of light they possess a beam of single wave length. Conventional sources of light have broad band emission. Monochromaticity is very much important in laser welding of materials as it determines the degree to which a laser beam can be focused. A monochromatic beam can be focused sharply than a broad bandwidth beam, as radius at the point of focus can be equivalent to the wavelength of beam [6].

2.1.3 Beam coherence

Coherence is a condition of light beam when a fixed phase relationship exists between two points of the same wave or between two waves. Laser beam has well defined beam coherence. The coherence phenomenon varies with space and time. So both coherence i.e. spatial coherence and temporal coherence are considered.

Spatial coherence occurs in the condition where the phase difference between two points on a wave front of an electromagnetic field remains constant with time. Even a single beam is

spatially incoherent; this usually describes constant phase relationships between two beams of light [6].

Temporal coherence refers to the condition where the phase difference between the two wave front of a light at a given point and time at the same point with next periodic time remains constant with time. The laser source is then temporally coherent over time.

2.1.4 Intensity and brightness

Laser beam has low divergence and high directional properties that facilitates the beam to be concentrated into a very small region, resulting in high energy density. But in case of an ordinary bulb light, the beam is radiated in all directions uniformly. Hence, only a small fraction of the emitted energy is available over a given area. As the distance from source increases, the intensity of light decreases.

Brightness is a basic property of the laser source. The brightness of a power source at a point is defined as the power emitted per unit surface area per unit solid angle. Brightness of a light source is always constant. For 1 W laser of line width 1 MHz, the brightness temperature is of the order of 10^{19} K [6].

There are different kinds of laser. Each one has different characteristics that depend on the active medium used for laser action. Various types of lasers are listed below:

1. Solid state laser
2. Gas laser
3. Liquid dye laser
4. Semiconductor laser
5. Free electron laser

1. **Solid state laser**

Solid state lasers normally use a host material made up of glass or insulating material in which active medium is embedded. Active medium is either dopant or acts as an impurity inside host material. The active medium present in host material actually participates in laser action but

the host material doesn't participate directly in this process [7]. Instead of interstitial impurity, substitution impurity comes into picture where the active material substitutes some of the atoms in the host material.

Solid state lasers may be continuous wave or pulsed beam types. At the same time most of the solid state lasers are controlled in beam mode which makes them unsatisfactory for various interference based requisitions as their coherence lengths are generally short. Then again, the significant energy produced in each one pulse makes them attractive to requisitions that require lot of energy in brief time. Common examples of solid state lasers incorporate the ruby, Nd:yag and Nd:glass laser.

2. Gas lasers

Gas lasers are the mostly used in the industry so far laser welding is concerned. The power levels range from several kilowatts to miliwatts. They can be operated either in continuous mode or in pulsed mode, with output frequencies ranging from ultraviolet to infrared. In gas laser an electric current is released through a gas to handle coherent light [8]. The gas laser was the first persistent light laser and the first laser to work on the principle of changing over electrical energy to a laser light output. Gas lasers utilizing numerous gasses have been assembled and utilized for some reasons. Basic sorts of gas lasers incorporate Helium–neon laser, Carbon dioxide laser, Argon ion laser, Copper laser and so on.

3. Liquid dye laser

Organic dye is used as the lasing medium in a dye laser, usually as a liquid solution. Compared to gas laser and solid state laser, a dye can usually be used for wider range of wavelengths. The wide bandwidth helps them to be used for tunable lasers and pulsed lasers. However, different dies can be used to generate different wavelengths with the same laser [9].

Now-a-days the laser dyes contain larger organic molecules which fluoresce. To emit stimulated radiation, the dye molecules are excited by the incoming light. In this state, the dye is transparent to the lasing wavelength and the molecules emit light by fluorescence. Suddenly the molecules will change to their triplet state within few micro seconds. In the triplet state, light is emitted by phosphorescence. The molecules absorb the lasing wavelength, making the dye opaque. Liquid dye also has extremely high lasing threshold.

Flash lamp pumped lasers use a flash for a very short duration, to deliver the large amounts of energy. Dye lasers with an external flash lamp can provide enough energy of proper wavelength into the dye with a relatively small amount of input energy, but in order to keep the triplet molecules out of the beam path the dye must be circulated at high speeds.

4. Semiconductor laser

Semiconductor lasers are widely used because they are cheap and compact in size. They consist of complex multilayer structures. In this laser accuracy should be more and design should be perfect. In order to generate new and improved designs, their theoretical description is important. The laser is a carrier inversion system which results in an electromagnetic polarization that drives an electric field [10, 11]. In most cases, the electric field is confined in a resonator, the properties of which are also important factors for laser performance.

5. Free electron laser

A free electron laser is a high speed laser that moves very fast in a magnetic field [12]. So, free electron acts as lasing medium in this case. The free electron laser has the maximum frequency of all the type. The frequency range can vary from microwave to visible spectrum, ultra violet and X-ray.

In free electron laser, a beam of electrons is accelerated in the pace of light. The beam passes through an undulator, in which a side to side magnetic field is handled by an periodic action of magnets with substituting posts over the beam path [12]. The direction in which beam moves is called longitudinal direction, while its perpendicular direction is called transverse direction. This show of magnets is prominently known as an undulator or a wiggler in light of the fact that it drives the electrons in the beam to wiggle transversely along a sinusoidal way about the hub of the undulator [13].

2.2 MECHANISM OF LASER FORMATION

Operation of the laser depends on the utilization and to some extent, manipulation of the naturally occurring transitions between the energy levels of a quantified system such as atom. Two fundamental concepts such as photon and stimulated radiation are very important to the invention of the lasers.

In Bohr-Somerfield model of atom, negatively charged electrons orbit along specific paths (orbital) around a positively charged nucleus. The positions of the discrete orbitals depend upon a complex set of conditions such as the number of electrons surrounding the nucleus, the existence of nearby atoms and the presence of electric and magnetic fields. Each orbital defines a unique stationary energy state in the atom. The atom is said to be in its ground state if all the electrons occupy the orbitals that have the lowest potential energies [14]. The electrons at the ground state can be excited to higher energy state by absorbing energy in various forms such as through vibration at elevated temperature, by collision with other atom or through absorption of photons.

For example, by the absorption of photons when the electrons are excited to higher energy state, they will almost immediately decay back to the ground state in about 10 ns and happens spontaneously. Spontaneous decay often results in spontaneous emission of photons. They have exactly the same frequency as the exciting photons. Light created from atoms may be in random direction but at well-defined wavelengths called "emission lines" [15]. These emission lines can intensify when more electrons are pumped to the higher energy state.

In an atom, some transitions are possible than the other. There are well established selection rules in quantum mechanics that predicts the probability of any given transition under various circumstances. This ultimately would determine the intensity of absorption of emission line. However, sometimes the excited atom may be trapped in an energy state forbidding it for any downward transition. So the atom can linger in this so called metastable state from micro to milliseconds range before decaying to a lower energy state.

The existence of metastable states can upset the thermodynamic equilibrium which normally prevails in atomic system. If enough electrons get hung up in a metastable state, its population would exceed the population of atoms in ground state. Thus creating a condition for "population inversion" [6], which is thermodynamically unstable. When more energy at higher energy state is available for an avalanche waiting to happen, all that needed is some kind of stimulation to set the downward transition. Fig. 3 shows the stimulated emission of radiation as a result of population inversion.

Before emission | During emission | After emission

Excited level — E_2

$h\nu$
Incident photon

ΔE

Ground level — E_1

Atom in excited state

Atom in ground state

$h\nu$

$$E_2 - E_1 = \Delta E = h\nu$$
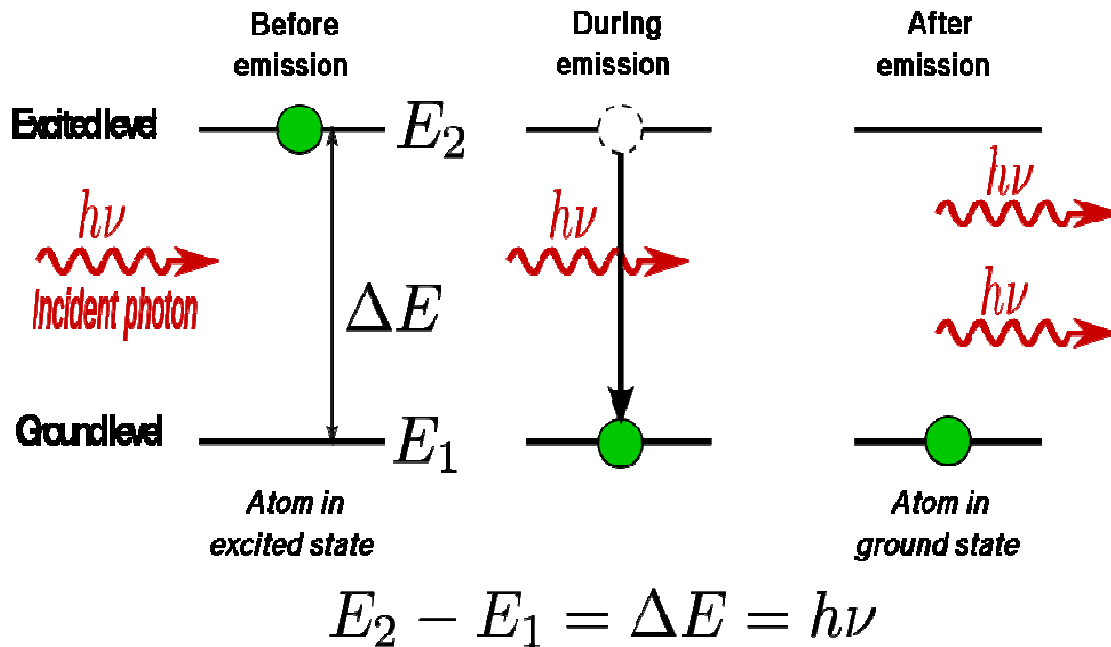
Fig. 3: Stimulated emission at population inversion [16]

To practically implement the phenomenon we have to take an example of Fabry-Perot interferometer. The Fabry-Perot interferometer consists of two parallel mirrors placed apart by a certain distance. The radiation suffers multiple reflections in between the mirrors. Under the condition, the light is said to be resonant with the cavity. The resonant condition transforms the interferometer into a highly selective filter. The selectivity depends on the reflectivity of the mirrors. At resonant wavelengths, the reflectivity inside the cavity can be very high and create an excellent feedback environment for the laser gain medium. Under the condition, the population inversion is high enough to overcome all the losses inside the cavity. Thus so called threshold condition [6] would be met and lasing action will begin. To couple light out of the cavity, one of the mirrors is usually made partially reflective.

2.3 Nd:YAG LASER PROPERTIES

Nd:YAG is a solid state laser. Nd:YAG is the acronym for Neodymium Yttrium Aluminum Garnet; Nd:$Y_3Al_5O_{12}$ which is used as the lasing medium. It consists of a host material which is crystalline solid doped with an active material whose atoms provide the lasing action. Nd:YAG laser consists of a single Neodymium. The dopant Neodymium which is triply

ionized substitutes a small fraction of the yttrium ions in the host crystal structure of the yttrium aluminum garnet as both are of similar size. Neodymium ion provides the lasing action.
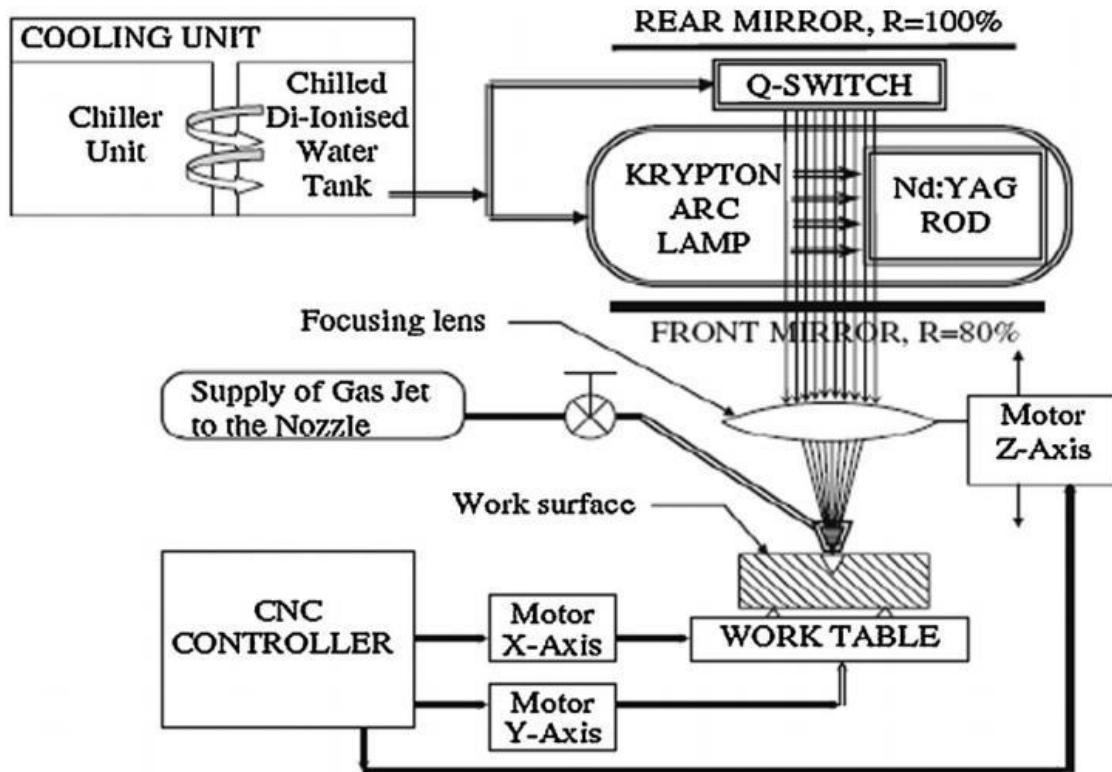
Fig. 4: Schematic diagram of Nd:YAG laser unit [17]

Nd:YAG lasers are optically pumped utilizing a flashtube. These are a standout amongst the most widely recognized sorts of laser, and are utilized for some distinctive provisions. Nd:YAG lasers regularly radiate light in infrared region with a wavelength of 1.064 μm [18]. Nd:YAG lasers work in both pulsed and continuous mode. Generally, pulsed Nd:YAG lasers are regulated by Q-switching mode. For highest population inversion in the neodymium ions, an optical switch is embedded in the laser cavity. The light wave can pass through the cavity, diminishing the population inversion in energized laser medium at maximum population inversion. In this Q-switching mode, output power of 250 MW and pulse duration of 10-25 ns

could be accomplished. The high-intensity pulses may be efficiently multiplied to create laser light at 532 nm [18].

Nd:YAG absorbs photon mostly in the bands between 730–760 nm and 790–820 nm. Xenon lamps are commonly used for pumping in Nd:YAG laser system. At low current densities krypton flash lamps have higher output than xenon lamps, which produce more light at around 900 nm. So krypton lamp is more efficient for pumping Nd:YAG lasers. The amount of the Neodymium dopant in the material varies according to its use. The doping is however smaller than the doping used for pulsed lasers. They can be distinguished by their color. The lightly doped CW rods are less colored, generally white, while higher doped rods are pink-purplish.

Nd:YAG lasers are used in manufacturing for different purposes in metals and plastics. They are widely utilized within industry for cutting and welding steel and different alloys. This is exceptionally suitable for automotive applications like cutting and welding steel where the power levels are regularly 1–5 kW [19]. Super alloy drilling which is mostly utilized for gas turbine parts utilizes pulsed Nd:YAG lasers. This is also utilized to make subsurface markings in transparent materials like glass. In aviation provisions, they could be utilized to drill cooling gaps for upgraded wind current. Nd:YAG lasers are also used in the non-conventional rapid prototyping process.

Properties of Nd:YAG with 1% Nd doping at 25 °C are listed below [19].

- Formula: $Y_{2.97}Nd_{0.03}Al_5O_{12}$
- Weight of Nd: 0.725%
- Charge state of Nd: 3^+
- Atoms of Nd per unit volume: 1.38×10^{20} cm^{-3}
- Wavelength of emission: 1.064 μm
- Fluorescence duration: 0.230 ms
- Modulus of elasticity: 3.17×10^4 Kg/mm^{-2}
- Poisson's ratio: 0.25
- Thermal expansion: 6.9×10^{-6} K^{-1}
- Thermal conductivity: 0.14 W cm^{-1} K^{-1}
- Specific heat capacity: 0.59 J g^{-1} K^{-1}

2.4   LASER WELDING

Laser welding is a high energy density welding process with specific advantages over conventional fusion welding processes. Laser welding is characterized with high welding speed, narrow heat affected zone and low distortion. One of the key features of laser welding is that without filler materials welding can be done. As the beam can be concentrated at a small area so it provides a concentrated heat source, allowing for narrow, highly penetrated welds. The process is frequently used in high volume applications, such as in the automotive industry.

2.4.1 Process description

The laser produced by the pumping is mainly of continuous wave. A Q-switch is used in order to produce pulsed waves from continuous type. The beam is delivered either by conventional beam delivery system to the welding portion or by Fiber optics beam delivery system.

Conventional beam delivery system is simple and consists of a movable reflective mirror with a convex lens. Generally the mirror is held at 45^0 to the incoming beam so as to deliver it in right angle to the original direction. Common materials used for mirrors include copper or molybdenum [20] without coating or with coating of silicon.

Optical fibers are generally used for transmission of laser beams directly from one location to another location. This system is generally used in optical communication where the power levels are low [21]. The basic components of fiber optic system consist of transmitter, transmission line and receiver.

To avoid temperature rise in mirror, beam expander is used. Sometimes for welding in different positions beam splitter is used which splits the beam in the desired direction. The beam is then transferred to the convex lens made up of Zn-Se, KCl or GaAs. The convex lens helps the beam to be concentrated at its focal point where high energy density can be achieved. Varying the position or the convexity of the lens the focal point position can be varied. So utilizing this advantageous effect we can generate defocused beam or focused beam at the metal surface and metal processing can be done accordingly [6].

The focused beam is concentrated at the joint of the two metals. However, due to small beam size, lasers are primarily used for butt joint and lap joint configuration. The two metals to be joined are configured properly on a clamp and the beam is allowed to travel along the joint. In this process either the worktable is constant and the beam traverses along the joint or the beam emergence is constant and the CNC operated worktable moves accordingly. Fig. 5 shows laser welding process with process parameters.
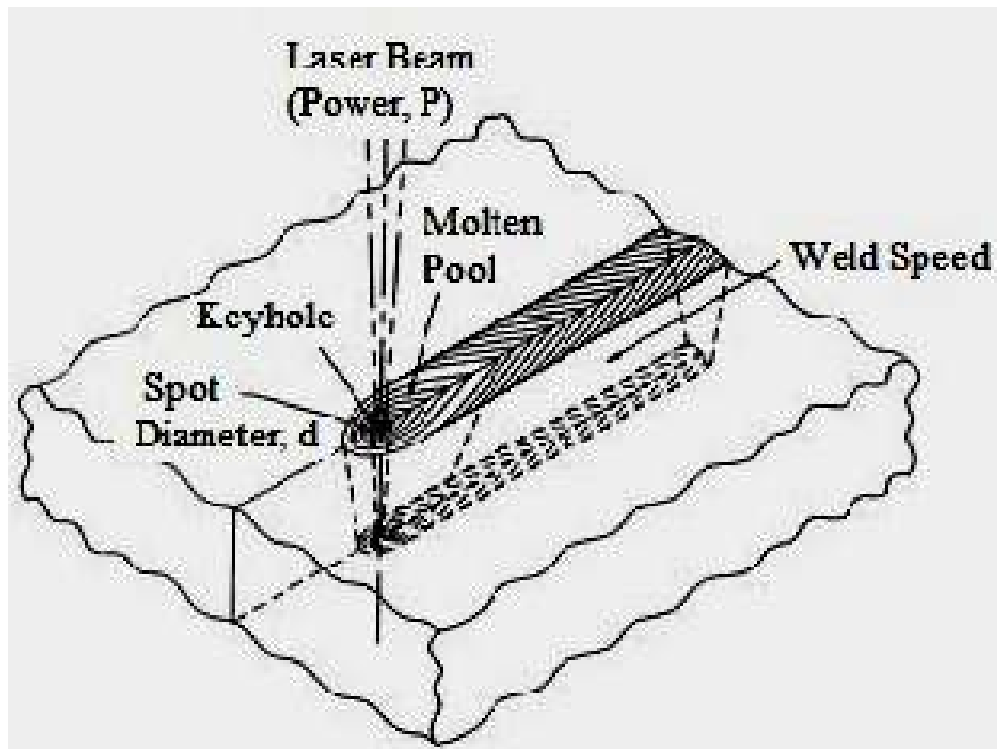
Fig. 5: Welding process by laser [22]

The power is supplied and the machining parameters in the laser machine are set carefully. Then the metals are clamped properly under the beam source. The length of traverse is set in the machine and the edge of the joint is taken under laser source. The whole system is controlled by computer. As soon as the start command is given by the computer the traversing of the laser starts from the one end of the joint and ends at the other end. This completes the laser welding of the particular metals.

2.5 MECHANISM OF LASER WELDING

A sequence of events happens when a laser beam falls on a metallic surface. A critical portion of the beam may be reflected away at first. A little portion of the beam is assimilated by the surface. The surface gets warmed and temperature increases. With rising temperature, the surface absorptivity increases, which further builds the temperature. This may result in localized melting and possible evaporation of the metal [6]. Such vaporization creates a vapor cavity in the metal. Laser welding may thus be one of the two forms:

1. Conduction mode
2. Keyhole mode

2.5.1 Conduction mode welding

Conduction mode welding comes into picture at power density less than 10^6 W/cm^2, in which vaporization of work piece is minimal [6]. In this process when the laser source is incident on metallic interface, some of the power gets absorbed by the metal and some reflects back to the surrounding. The absorbed power melts the surface and welding takes place. So the penetration of welding completely depends on the power of laser beam and the distance of the initial point of contact of laser beam. Thus welding takes place through conduction. Convection also helps in forming weld pool. The conduction mode welding has low welding depth and small aspect ratio compared to keyhole welding. Coupling efficiency is less in this welding. But weld bead generated in this welding is very smooth. Laser welding of thin work pieces like foils, wires, thin tubes, enclosures etc. are being done by conduction mode welding [23]. A typical configuration of conduction mode welding is shown in Fig. 6.
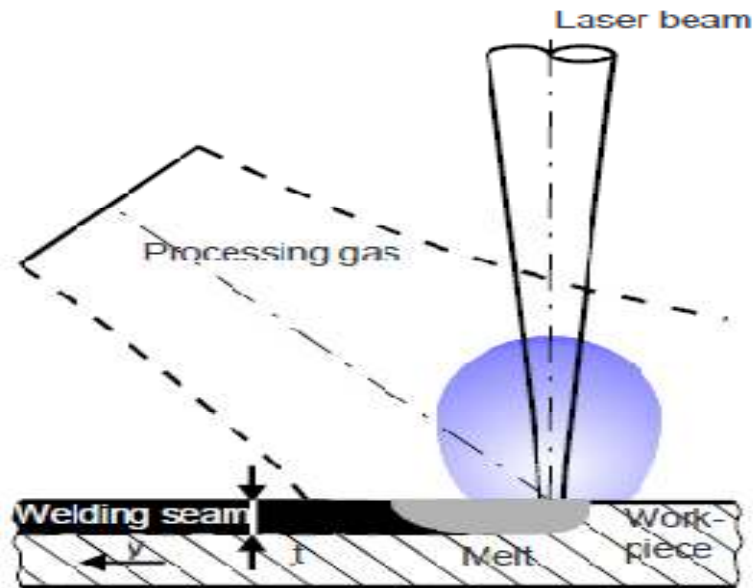
Fig. 6: Conduction mode welding [24]

2.5.2 Keyhole mode welding

At very high power density of 10^6 W/cm^2, keyhole cavity is formed by vaporization of specific portion of the metal. The keyhole cavity is encompassed by liquid metal which thus encompassed by strong base material. The liquid material around the keyhole fills the cavity as the beam is traversed along the joint [6]. The cavity contains vapor, plasma or both. Powers at play that have a tendency to crumple the keyhole cavity are as follows:

1. Surface tension at the interface between the molten metal and vapor or plasma.
2. Hydrodynamic pressure of the molten metal.
3. Hydrostatic pressure of the molten metal.

The forces are however balanced by
1. Vapor pressure in the cavity that repels the molten metal towards periphery which is greater than atmospheric pressure by about 10%.
2. Ablation pressure of vaporized material as it leaves the keyhole strengthening the vapor pressure.

When the scan speed is zero or when the beam is stationary, the keyhole cavity grows steadily due to vaporization. But when the beam starts moving, it is difficult to achieve steady state condition. So the cavity tends to collapse soon. But under movable condition of the beam the steady state can be achieved [18]. In this case the beam has to be moved with the cavity at a speed determined by the beam so as to defend collapsing of the cavity. As the beam proceeds it tends to push the material behind the cavity which happens due to flow of molten material around cavity or due to vapor pressure. The driving force for flow of molten material through keyhole cavity is due to ablation pressure of vapor or surface tension of molten material. But the later force is greater than the surface tension as the interface temperature is almost same as equilibrium evaporation temperature. Maximum pressure occurs at vapor-liquid interface and it decreases gradually to the side of the keyhole. Under steady state condition, the cavity moves uniformly with all isotherms. Fig. 7 indicates keyhole welding process in equilibrium condition.
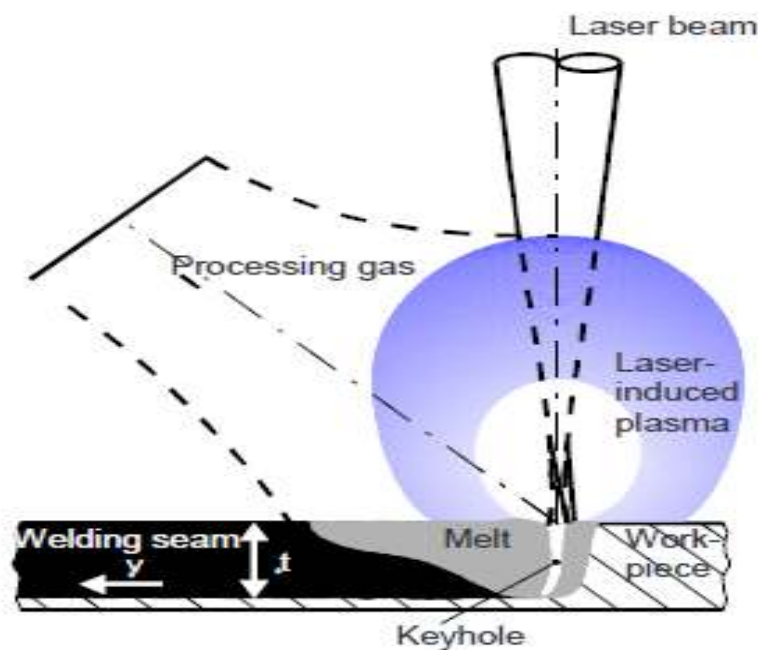
Fig. 7: Keyhole welding [25]

The keyhole configuration is assumed to be cylindrical shape. But as the vapor pressure is the function of depth of cylinder so vapor pressure varies with depth. The variation of vapor pressure with keyhole width results in tapering of the cavity towards bottom. It causes vapor to emerge at the opening as axial jet. But the axis of keyhole is bent towards the work piece travel direction. So the top surface of the molten metal develops a tear drop shape with length to width

21

ratio of about 10. The molten pool is circular at low welding speed. At the higher speed the tear drop shape becomes more pronounced. The width of the molten pool decreases at the higher welding speed.

When the power of the laser source is low, the vapor pressure produced in the keyhole is less than the combined effect of surface tension, hydrostatic force and hydrodynamic force. Hence the keyhole collapses and sudden drop in penetration occurs. So the weld pool becomes hemispherical shape. Keyhole welding is more efficient than conduction mode welding, since in conduction mode welding more light is reflected back to the surroundings. Conduction mode welding has depth to width ratio of about 3:1 whereas for keyhole welding it is up to 10:1. Absorption of energy in keyhole welding occurs by two principal mechanisms as mentioned below.

1. Inverse bremsstrahlung absorption of the plasma
2. Fresnel absorption at the cavity walls

The two mechanisms of keyhole welding specified above occur more or less simultaneously. The energy coming from source gets entrapped in the keyhole, thus vaporizing the material. The entrapped energy results in increase of absorption than absorption in conduction mode welding.

1. Inverse bremsstrahlung absorption of the plasma

Inverse bremsstrahlung is the absorption of electromagnetic radiation as a result of sudden acceleration of charged particles in electric field. In this absorption process a portion of the vaporized metal is ionized by high energy density to form plasma which further ionizes the incident beam. Thus in this process the temperature of the cavity increases which tends to increase the absorptivity. The plasma formation in keyhole welding is shown in Fig. 7. Since the middle of the keyhole is much more hot than the walls, the majority of the beam energy is retained inside the cavity, and after that coupled to the keyhole wall through conduction and radiation [26].

2. Fresnel absorption at the cavity walls

In Fresnel absorption laser beam is spread along entire keyhole length. When the beam is incident in the cavity, multiple reflections take place inside the keyhole wall. The beam entering into keyhole is reflected repetitively at walls until whole energy gets absorbed inside cavity [27]. With Fresnel absorption high welding depth and high aspect ratio can be achieved. It has high coupling efficiency.

2.6   LASER WELD CHARACTERISTICS

Cracking in weldment is an important factor to be considered for quality analysis. Hardenability and susceptibility of the hardened structure are more sensitive to cracking. Hardenability in a metal occurs due to faster cooling. In stainless steels hardenability occurs as a result of martensitic formation. Faster cooling produces higher hardness and hence hardened structure is more susceptible to cracking.

Na et al. [28] studied nonlinear identification of laser welding process. Here a standard diode laser welding system was established and a series of experiments were performed to investigate correlations between welding parameters and the weld pool geometry. Continuous hammerstein identification methodology was used to demonstrate significant nonlinearity in the diode laser welding process. The hammerization identification process includes 2 steps. To detect the linear dynamics and the static nonlinear function of the input from step responses with different step levels and to identify the parameters in the static nonlinear function. Also error based identification strategy was implemented to detect nonlinearity which is rather simple one. For identification of nonlinearity both methods were applied to the diode laser system and it was found that in each case, the model takes the reciprocal of the welding speed as the input and the top side surface width of the weld pool as the output.

Seang et al. [29] studied effect of Nd:YAG laser welding parameters on the hardness of lap joint. They tried to find microstructure overview and micro-hardness of weld zone both experimentally and numerically by simulation. Higher volume of martensite inside the FZ and the HAZ caused higher hardness insides these zones and no softening zone found in laser Nd: YAG on sheet metal of dual phase steel DP 600. In order to prevent crack and fracture formation

scan speed, focal position and power of Nd:YAG laser should be controlled. Interaction between various process parameters were observed and it was found that the laser parameters have strong influence on the hardness along the depth of the weld bead but no influence on the hardness inside the softening zone.

Wang et al. [30] studied bending properties and fracture behavior of Ti-23Al-17Nb alloy laser beam welding joints. Here longitudinal three point bending method was used to know ductility at bending of the laser welded joint. Again fracture behavior of the weld zone comprises of crack distribution and trace of fracture surface. It was clear from experiment that as bending ductility increases the heat input by the laser beam welding decreases. If columnar structured crystals were uniform then it was found to retain less ductility. The cracking propagated transgranularly and the fracture surface had cleavage mode as was found from fractography analysis. Again it was observed that when metal grains are fine and irregular, plastic deformation takes place with better crack propagation resistance and higher fracturing strains. To avoid formation of coarse and oriented columnar crystals heat input should be reduced.

Sun et al. [31] experimented on laser beam welding of ferritic stainless steel for the motor vehicle exhaust 409L. Here 1.5 mm thick 409L stainless steel was taken for laser welding in CO_2 laser. Before welding it was preheated by argon arc welding. The laser welding of stainless steel showed various advantages such as HAZ was narrow and the grain growth degree was small. Moreover, it could well satisfy motor vehicle exhaust pipe production.

Shenghai et al. [32] considered the welding joint properties of hybrid laser-TIG welding on thick plate. Here laser-TIG welding was utilized on thick plate of high quality low composite structural steel 10CrNiMnMoV. It was presumed that hybrid welding innovation can lessen the utilization of laser power and aspect ratio of weld throughout cross breed welding. So the gas has a tendency to escape effortlessly while welding thick plates and subsequently porosity diminishes. It was found that welding joint was better and its hardness was higher than base material. The assembling clearance and misalignment versatility of weldment had enormous upgrades using the hybrid laser-TIG welding technology to weld thick plates.

2.6.1 Dissimilar material welding

Welding of metals and alloys is an accomplished subject, dissimilar welding represents a major scientific and technical challenge. Developing new technologies progressively require dissimilar metals and alloys to be joined. Most metals and alloys are extremely weldable either in conduction or keyhole modes. This section describes the literature survey of the broad topic of interest namely the welding of dissimilar materials by laser welding. It gives a brief description of the welding process by laser welding.

Khan et al. [33] studied laser beam welding of dissimilar ferritic and martensitic stainless steels in a butt joint configuration. Here they took AISI 430F and 440C stainless steel for laser welding. Here the main objective of the paper was to avoid micro crack formation in the laser welding by following pre and post weld heat treatment and it was found that the heat treatment successfully avoided micro crack formation. Again laser power, scan speed and line energy input were optimized by generalized full factorial design using design export software. It was found that laser power and scan speed were the most significant factors in determining the weld crack. Formation of keyhole resulted in change in weld geometry within a certain range of energy input. After the upper limiting value, generation of upper keyhole plasma plume only contributed to the change in shape of the weld bead.

Sokolov et al. [34] analyzed laser welding and weld hardness of thick section S355 structural steel. This study investigated the performance and potential of deep penetration laser welding of S355 EN 10025 structural steel of 20 and 25 mm thickness with a high power fiber laser at power levels of 12–30 kW. It was concluded that increase in scan speed decreased HAZ and increased hardness. Also it was clear that as laser power increased hardness of weld zone decreased and HAZ increased. The difference between weld hardness and base material hardness could be decreased by decreasing laser scan speed and vice versa.

Khan et al. [35] investigated on laser welding of martensitic stainless steels in a constrained overlap configuration. Experimental studies were concentrated on the effects of scan speed, laser diameter and laser power. The contour plots and energy density plots were drawn for

determining relationships within various factors. They concluded that laser power and scan speed were two most significant factors affecting weld bead geometry and sheer force of the weld zone. Pulse diameter had least effect on weld geometry and shear force on weld zone. But its interaction effect beard a good value in case of weld bead and sheer force of laser weld. It was clear that welding resistance input increased with welding density up to certain limit. But as the welding density crossed the limit the density was utilized to increase penetration only. In SEM it was observed that the HAZ microstructures obtained in inner and outer shells of AISI 416 and AISI 440FSe were different from each other. In inner shell zone, microstructure possessed both primary and secondary Cr-rich carbides in tempered martensitic matrix but in outer shell the softening of HAZ took place due to presence of ferritic structure.

2.6.2 Austenitic plate welding

Austenitic stainless steels are decently welded and the issue of hot cracking of welded joints is constrained. Decrease of carbon content in austenitic steels and consumables prevents the inter-grain erosion of welded joints. High thermal expansion is the main cause for thermal distortion in welding, especially in the welding of thin plates [36]. Past investigations of the weldability of stainless steels show that the most elevated nature of welded joints of austenitic stainless steel sheets is guaranteed just by laser welding. The surfaces of laser welded joints are smooth and with no undercuts and the reinforcement height is insignificant. The butt joints of austenitic steel sheets welded by the laser at optimal parameters are of high caliber, without any internal imperfections and the length of HAZ is less. The mechanical properties of laser welded butt joints of austenitic steel sheets are not lower than the properties of the base material.

Sathiya et al. [37] designed a streamlined model for laser butt welding process parameters utilizing artificial neural network and genetic algorithm for butt welded AISI 904L super austenitic stainless steel. Full factorial design was employed to carry out experimentation. Artificial neural networks model was produced to build the relationship between the laser welding data parameters and response parameters. Beam power, focal position and scan speed were taken as input parameters whereas depth of penetration, beam width and tensile strength were taken as responses for different shielding gases. The great understanding between the hypothetically anticipated (GA) and experimentally obtained tensile strength, depth of

penetration and bead width affirms the appropriateness of these evolutionary computational procedures for optimization of process parameters in the welding methodology.

2.6.3 Carbon steel plate welding

Low carbon steel is not supposed to harden. In theory, there is just not enough carbon in low carbon steel to allow it to harden. Fortunato et al. [38] simulated numerically nanosecond pulsed laser welding of eutectoid steel components. They took two eutectoid carbon steel grades and welded it by micro seam laser. They welded these materials by seam welding because in this welding process welding will end at the starting point of welding so that micro crack will not form as these materials are sensitive to crack formation. The simulation of the micro welding was done in order to evaluate the weld pool dimension and heat affected zone extension. The process was found to be superior as it had high manufacturing rate, high thermal gradient, minimal distortion and consumes minimum energy compared to other fusion welding processes.

2.6.4 Modeling and optimization of laser welding parameters

Various process parameters which influences the welding process was studied and how these parameters were optimized at different conditions were stated critically. It also presents a review of the simulation of process parameters in welding. The advantageous effects and limitations of laser welding over other welding processes were illustrated. Some of the literatures from journal are presented below.

Pan et al. [39] optimized process parameters of Nd:YAG laser welding onto magnesium alloy via Taguchi analysis. The optimized welding parameters were determined by evaluating ultimate tensile stress. Six welding parameters such as shielding gas, laser energy, convey speed of work piece, point at which the laser was focused, pulse frequency and pulse shape were taken at L_{18} orthogonal array combination to follow Taguchi methodology. The optimal result was found to be 2.5 times than original set for laser welding. The optimization of Mg alloy butt welding was studied using Taguchi methodology. It was found that the pulse shape and the energy of the laser contributed the most to thin plate butt welding. It was concluded that Ar as the shielding gas, laser power of 360 W, scan speed of 25 mm/s, laser focus distance of 0.05 mm, pulse frequency of 160 Hz, and type III pulse shape bears optimized results. The ultimate tension stress was the maximum at an overlap of the welding zone of approximately 75%.

Acherjee et al. [40] displayed and dissected concurrent laser transmission welding of polycarbonates utilizing FEM and RSM joined together approach. The destination of the examination is to study the impacts of process parameters on the temperature field and weld bead measurements. By ANSYS the thermal field is simulated by solving a diffusion equation and accepted with exploratory results. The second order Equation developed by RSM determines both relationship between response and input parameters and also levels of significant factors. It was found that all the response parameters taken increase with laser power and welding time.

Padmanaban and Balasubramanian [41] optimized laser beam welding process parameters to attain maximum tensile strength in AZ31B magnesium alloy. The process parameters considered were laser power, scan speed and pulse diameter. In RSM an empirical relationship was established between input and output parameters. The design was created taking three level three factors central composite design with full replication. Using RSM the parameters were optimized and it was found that laser scan speed has greatest influence in determining tensile strength of AZ31B magnesium alloy and the influence decreases to laser power and focal position respectively.

Pan et al. [42] improved different quality attributes through Taguchi technique based grey analysis. The setting of laser parameters are improved for combining various quality qualities into one incorporated numerical worth called grey relational grade. The machining parameters taken incorporate shielding gas, laser energy, scan speed of the work piece throughout welding, focusing position, frequency of the drive laser and pulse shape of laser. High ultimate tension stress, little HAZ, large welding depth to width ratio and low surface roughness in laser welding were considered as quality attributes for titanium alloy plate.

Muhammad et al. [43] optimized and modeled spot welding parameters with simultaneous multiple response consideration using multi-objective Taguchi method and RSM in plate thickness of 1.5 mm under different welding current, weld time and hold time. The optimization method considered the multiple quality characteristics namely weld nugget and heat affected zone, using multi-objective Taguchi method. These parameters were optimized using Taguchi design with L_9 orthogonal array. The optimum value was analyzed by means of MTM,

which involved the calculation of total normalized quality loss (TNQL) and multi signal to noise ratio (MSNR). The order in which the input factors affected the response were weld current followed by weld time and hold time.

2.7 FACTORS AFFECTING LASER WELDING

Now-a-days in industry the quality of the weld plays an important role. For acceptance in the industry, the quality should attain a threshold value. More quality means more demand. The parameters of laser welding are very important in determining the quality of the weld. So the parameters should be controlled properly in order to find welding of good quality. Hence consideration of parameters is very important in laser welding. The major parameters that influence laser welding are listed below.

1. Beam power and traverse speed
2. Beam characteristics
3. Gas shielding
4. Ambient pressure
5. Location of focal point relative to the work piece surface
6. Joint configuration

2.7.1 Beam power and traverse speed

Fig. 8 shows the variation of weld penetration with welding speed and laser power. It is clear that as the scan speed increases the penetration decreases and vice versa. The penetration depth decreases almost exponentially with welding speed. This can be explained as the scan speed increases a certain portion of the area is exposed to laser for very small time. So much of the energy can't be concentrated at that point. Hence penetration decreases. Fig. 8 also indicates as the laser power increases the weld penetration increases.
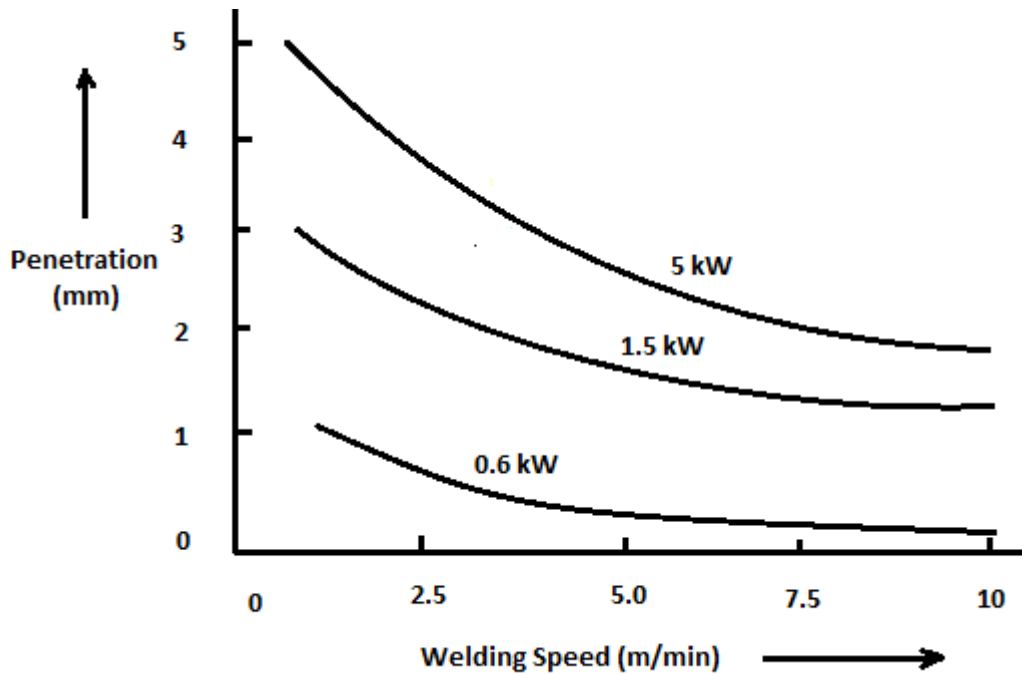
Fig. 8: Effect of welding speed and power on penetration [6]

A peculiar graph comes into existence when depth-to-width ratio is plotted against scan speed. Depth-to-width ratio increases with increasing traverse speed and then decreases. This may seem to be against Fig. 8. But when scan speed is less, the width of the weld zone increases simultaneously with penetration. Fig. 9 shows the variation of depth-to-width ratio with welding speed. Generally results obtained from low-power laser welding, lower than 5 kW cannot be estimated to high power welding, say 20 kW [15]. This can be explained by the difference caused by plasma shielding effects resulting from either high power densities or high evaporation rates that cause an enhanced plasma formation.
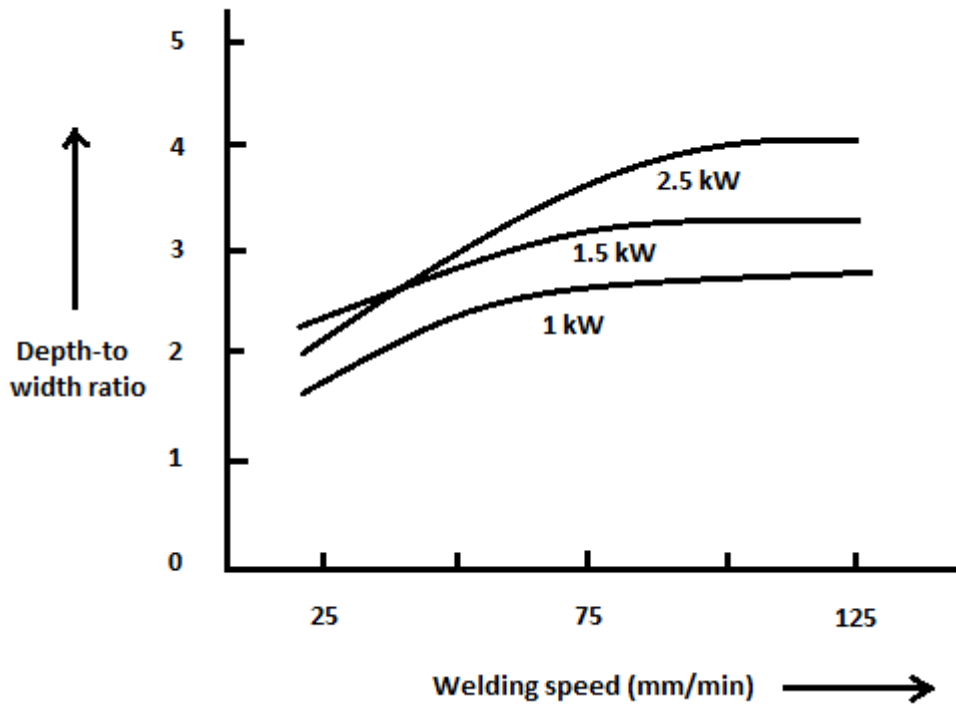
Fig. 9: Effect of welding speed on depth-to-width ratio [6]

2.7.2 Beam characteristics

Beam stability, beam mode, polarization of beam affects the laser welding process. The effects of these parameters on the welding process are discussed below.

1. Beam mode

The beam mode has significant effect on the weld bead shape. Concentrated shape of the TEM_{00} mode results in higher depth to-width ratio than higher order modes. The TEM_{00} mode results in a smaller focused beam radius which delivers a large amount of energy density. As the spot size of multimode beam is large enough, so it is more suitable for butt welding application in which the gap between joints is significant.

2. Beam stability

Beam stability can be defined as the repeatability of the beam characteristics. It helps in maintaining weld quality. Variation of beam characteristics, such as variation in power, mode,

absorption coefficient etc. affects the quality of welding. So in order to find welding of constant quality, beam stability should be controlled.

3. Beam polarization

The basic concept of beam polarization is discussed. The influence of beam polarization on the welding process depends on both the material and welding condition.

4. Pulsed beams

Both pulsed and continuous wave beams are used for welding, with pulsed beams being more suited for spot welding while continuous wave beams are more suited for continuous weld. Pulsed beams can also be used for continuous welds if the pulses are made to be overlapped each other. For keyhole welding the beam should have higher power.

2.7.3 Gas shielding

In laser welding, a shielding gas may be used for one or more purposes as mentioned below:

1. To blow away the vapor and plasma formed, enabling the beam to reach its target.
2. To provide a protective environment for the weld pool.
3. To protect the focusing lens.

Generally for laser welding He and Ar shielding gases are used. Argon shielding gas is used for laser welding with small to medium power laser. The higher density of the Argon gas makes it preferable for low power laser as it shields heavily compared to Helium gas. Again the surface produced by Argon shielded welding is smoother than Helium shielded welding.

Helium is used as shielding gas for high energy laser welding process. The higher ionization potential of Argon gas makes it suitable for high energy laser operation because for plasma formation in this case higher energy is required. But as the density of the Helium gas is very low so a large amount of gas should be supplied during welding process. The requirement of gas flow rate during welding process is shown in Fig. 10. The figure shows the effect of plasma suppression helium gas flow rate on the depth of penetration in plain carbon steel [6].

Nitrogen has least application as shielding gas in laser welding as Nitrogen usually traps to the weld zone and forms nitride which is brittle.
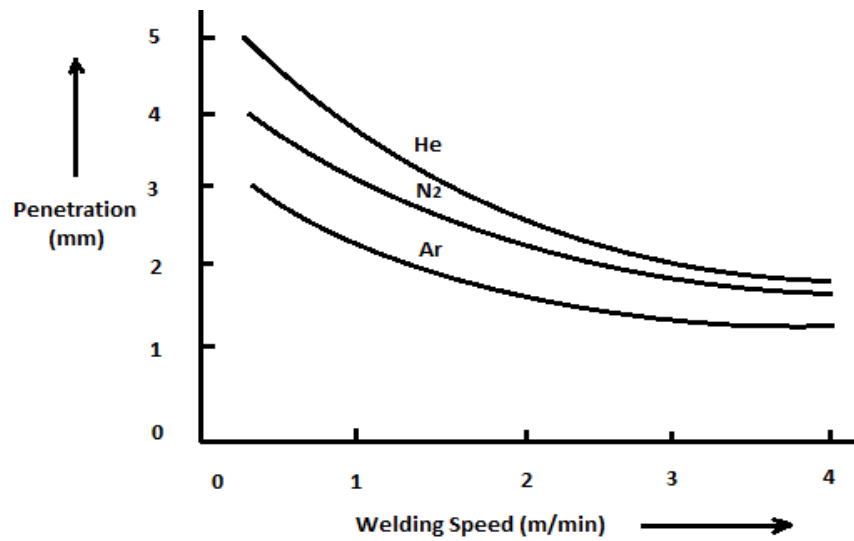
Fig. 10: Effect of shielding gas on penetration [6]

When gas flow starts, the welding is limited to conduction mode welding only. Up to a certain rate of gas flow, the energy of laser is utilized to form plasma. At a certain point of flow rate the conduction mode welding changes to keyhole mode welding as plasma enhanced energy coupling phenomenon comes into picture. Beyond flow rate of 40 L/min, the gas is energetic enough [6] to remove material from molten pool resulting deep bead. Fig. 11 indicates the effect of gas flow rate on penetration of welding.
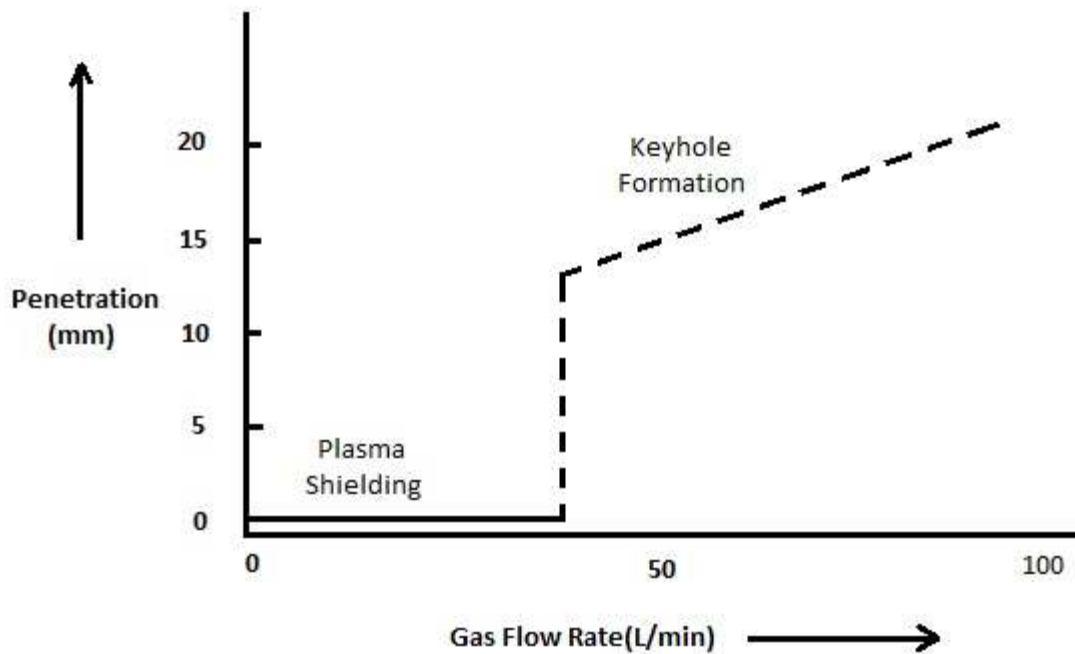
Fig. 11: Effect of gas flow rate on penetration [6]

The distance of nozzle from the plasma plays an important role in determining quality of weld. Initially as the distance increases, the penetration increases. This occurs as at very low distance plasma enhanced energy coupling is not very successful. The penetration reaches maximum at certain distance of the nozzle and then decreases dramatically as nozzle distance increases. This is due to more energy gets radiated to surroundings.
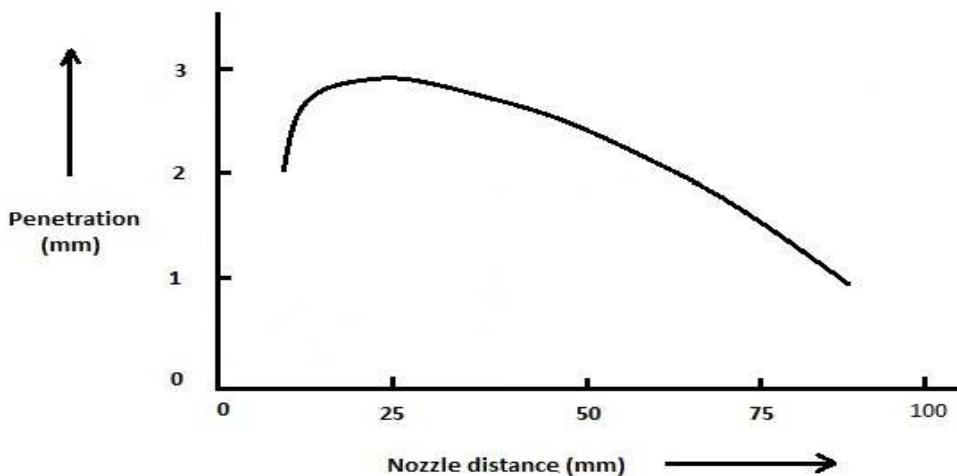
Fig. 12: Effect of nozzle distance from plasma with penetration [6]

2.7.4 Effect of ambient pressure

The ambient pressure also affects the welding quality. At lower ambient pressure the amount of plasma formed is reduced. Below a pressure of about of 5 Torr, the plasma is so small in size that no significant change is observed with further reduction in pressure. With decreasing pressure the penetration increases and pool width decreases. If the welding process will be operated in vacuum condition, the process efficiency can be increased 30-40% [6].

2.7.5 Beam size and focal point position

In laser welding, the position of focal point relative to work piece surface determines the beam size on the work piece. Depending on the beam size the penetration and weld width can be regulated. The optimum laser diameter obtains higher penetration and lower bead width. So at this point the depth-to-width ratio will maximum. Sometimes compromise should be followed for penetration and bead width.
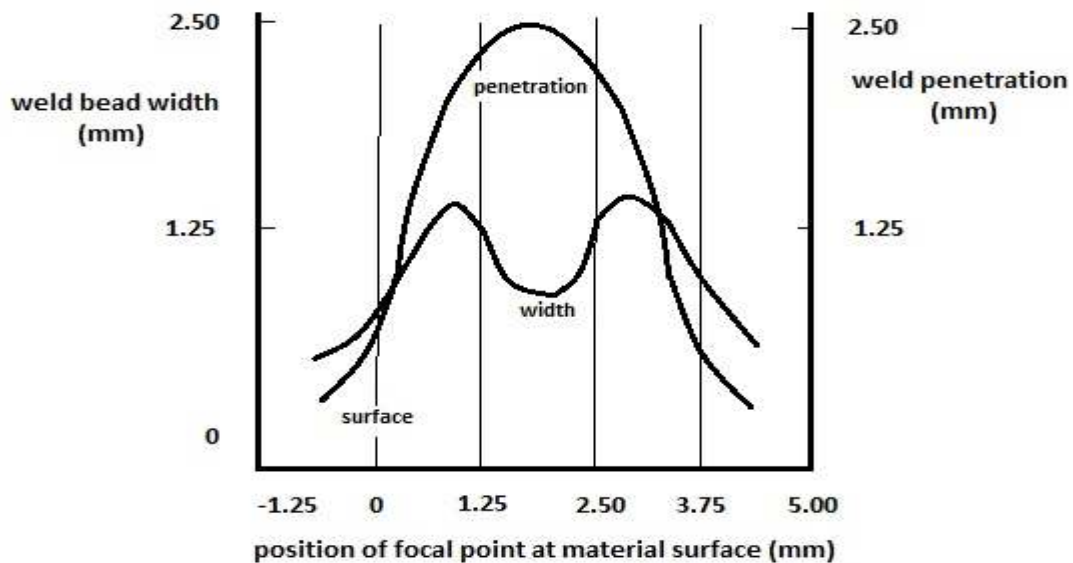
Fig. 13: Effect of focal point position with penetration and weld bead width [6]

2.7.6 Joint configuration

In laser welding various types of joint configuration are used. As the beam diameter of laser is very low, butt joint configuration is inefficient to be used. This is because most of the laser source passes away through the gap. Hence lap joint configuration is mostly used in laser welding. However, for butt joint, butt gap should be less than 10% of thickness of thinner metal [6] in order to avoid passing of laser through gap. This problem can be minimized by using defocusing laser beam at the interface.
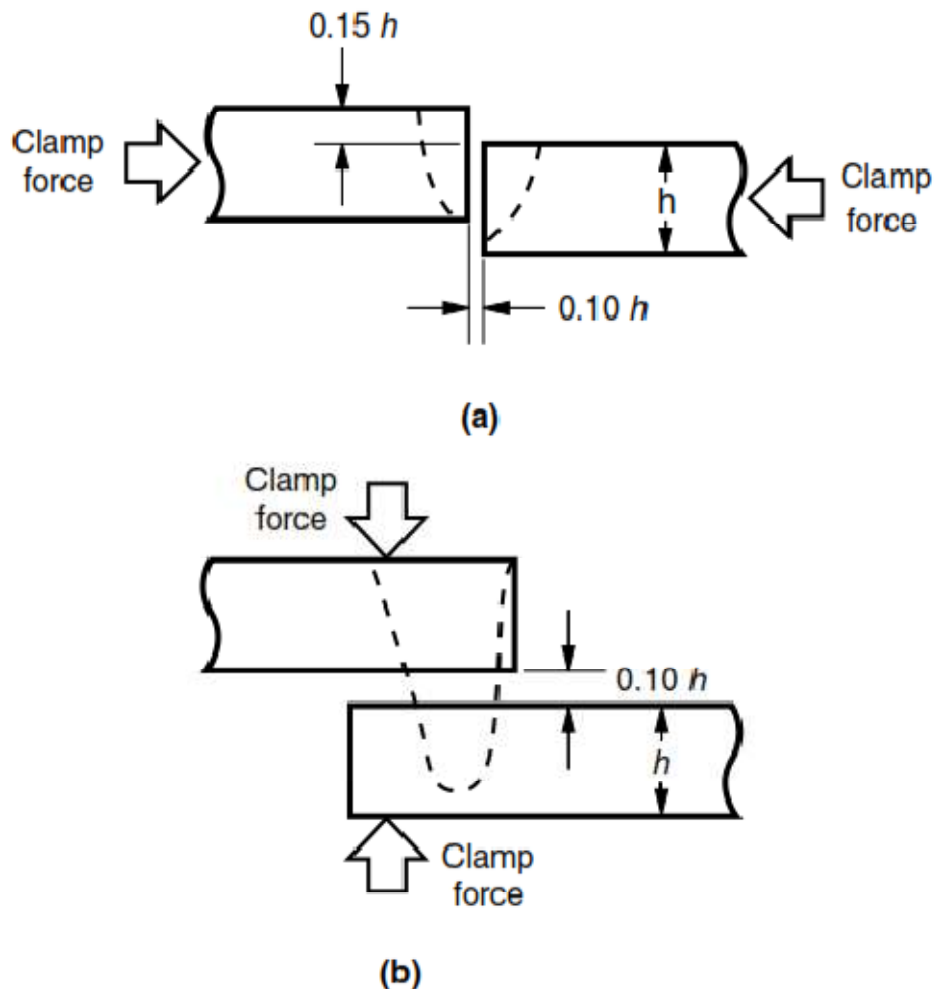
Fig. 14: (a) Butt joint and (b) Lap joint specification in laser welding [6]

The joint fitting requirement for lap joint is easier than butt joints since in the lap joint, the laser beam is made to penetrate through one piece into the underlying components. Lap joints are more appropriately used when the upper component is relatively thin.

2.8 ADVANTAGES AND DISADVANTAGES

Laser welding has both advantages and disadvantages. But advantageous effects dominate over disadvantageous effects. So this process is widely utilized in metal working operations in industry. Some of the advantages and disadvantages in laser welding are illustrated below.

2.8.1 Advantages of laser welding

1. The welding formed by laser is clean enough than any other welding. It incorporates very small contaminates from surrounding.
2. Laser welding has lowest distortion. More the laser stability, lower will be distortion.
3. Laser welding is a faster welding process. A scan speed of 20 m/min can be achieved by laser welding.
4. The materials which are difficult to be welded van be welded by laser. Aluminum which is very difficult to be welded can be welded by laser. Very hard materials come in this domain also.
5. Heat Affected Zone in laser welding is very narrow as a concentrated energy is supplied for less time by laser.
6. The welding process can be automated
7. Small size products with very narrow interface can be welded successfully by Laser.
8. Laser welding is suitable for heterogeneous materials having different physical properties
9. It doesn't require filler material.
10. It doesn't require vacuum.
11. Laser beam can be supplied to different work stations at a time by using switch device.
12. It is noncontact process. So the least mechanical stress is induced in the work piece.
13. Due to keyhole welding, penetration of welding is the maximum. So depth-to-width ratio of welding maximizes.
14. Bead width of welding is very narrow compared to other welding process.
15. Very high precision welding. Close tolerance and excellent repeatability.
16. Laser is not affected by the presence of any magnetic field.
17. Electrode is not required. Production cost is less.

2.8.2 *Disadvantages of laser welding*

1. The equipment cost of welding is expensive.

2. Thick metal plates can't be joined. Up to 5 mm thickness can be welded by laser.

3. Reflection of laser in welding process is hazardous to health.

4. Skilled worker is required for operating laser equipment.

5. Energy conversion efficiency is too low.

6. Energy consumption of the machine is too high.

CHAPTER 3

EXPERIMENTAL PROCEDURE

3.1 MATERIAL SELECTION

AISI 316L stainless steel and AISI 1552 stainless steel were selected for laser welding. AISI 316L stainless steel was cut to dimension of 50 mm x 30 mm x 2.5 mm and AISI 1552 stainless steel was cut to dimension of 50 mm x 30 mm x 2.0 mm. 16 samples for each material were cut to the aforesaid dimension. Both the materials were undergone XRF test to know the chemical composition. The chemical compositions of both the materials are given in Table 1.

Table 1: Composition of AISI 316L and AISI 1552 (Weight %)

Composition	C	Si	Mn	Ni	Cr	S	P	Cu	Fe
AISI 316L	0	0.529	1.551	11.37	17.026	0.007	0.054	0.22	66.772
AISI 1552	0.5	0.169	0.583	0.08	0.064	0.012	0.02	0.17	95.892

3.2 Nd:YAG LASER BEAM WELDING

The laser has some unique characteristics. The laser beam is coherent, collimated and can be concentrated at a point. So the energy density produced at the concentrated point is very high. This advantage of laser is used for welding of stainless steel. Small power Nd:YAG laser is used for welding thin plates. Smaller kerf width, micro-size holes, narrower heat affected zone and better cut edge kerf profile can be obtained in Nd:YAG laser beam machining.

Here in this project 200 W Nd:YAG laser was used for welding of AISI 316L stainless steel and AISI 1552 stainless steel in lap joint configuration. Before welding the samples were grinded properly by manual grinder in order to eliminate burr and oxides present over it. After grinding the samples were adjusted to their proper dimension and surface finish was achieved.

Again all the samples were cleansed by degreasing elements like spirit to remove any greasing material present on the surface. This is very important for the samples to be degreased because any greasing element present on the surface of the sample decreases the absorptivity of the laser.

As our objective of the experiment is to do welding in lap joint configuration, so the samples must be welded at the exact corner interface. Also as the weld width of the joint is very

small so the interface of the materials should be exposed at the right angle to the laser source. In order to achieve this one mounting made up of wood with inclination at 45^0 was prepared. The inclination surface was provided with pins in order to clamp the two materials to be welded. The mounting set up was made up of wood. Fig. 15 shows the mounting with clamping. Generally, the mounting had two functions given below.

1. To expose the joint interface to be welded at 90^0 to the laser source.
2. To clamp the two samples with pressure by the pins provided in it so that it can withstand the impact force applied by the laser at the time of welding.

Fig. 15: Mounting with clamp

The experiment was performed focusing the Nd:YAG laser on the interface of AISI 316L stainless steel and AISI 1552 stainless steel. The specification of the used laser beam is presented below:

1. Average laser power: 200 W
2. Maximum pulse energy: 10 kW
3. Maximum scan speed: 1.5 m/min
4. Maximum pulse diameter: 2 mm

For finding effective hardness of the weld zone and HAZ of the experiment, certain laser parameters were made constant and some were varied in a range. The constant parameters set in the machine are given as:

1. Pulse energy: 25 J
2. pulse power: 5 kW
3. pulse duration: 5 ms

The process parameters which are to be optimized were set in levels in the machine range. Each parameter had 4 levels. The effect of these process parameters were considered for evaluation of effective response. The process parameters with their respective levels are shown in Table 2.

Table 2: Process control parameters and their limits

Parameters	Unit	Level(1)	Level(2)	Level(3)	Level(4)
Scan speed	mm/min	30	45	60	75
Pulse diameter	mm	0.3	0.6	0.9	1.2
Pulse frequency	Hz	1	3	5	7

The samples were set on the mounting and clamped properly by the pins. The mounting in turn was fixed on a CNC motion table. The machine was switched on and required laser parameters were set by the computer. The length of the joint interface was measured and set in the computer as scan length. In this experiment, scan length was set to be 25 mm. The CNC table is motionless and the laser head moves over the joint by the scan length as the process starts. The process continued for all 16 sample pairs set according to L_{16} orthogonal array of Taguchi design. The setup of laser welding is shown in Fig. 1 and the final samples produced after welding were shown in Fig. 16.

Fig. 16: Welded samples

3.3 HARDNESS MEASUREMENT

In this work, hardness of weld zone was taken as one response parameter. Vickers hardness measuring machine was used to measure hardness. The Vickers test is more frequently used than other hardness tests since the required calculations are independent of the size of the indenter and the indenter can be used for all materials irrespective of hardness. It measures macro-hardness of the work piece.

As the indenter of Vickers machine is pyramidal shape so it is difficult to enter exact interface point of the welding which is very narrow. Hence measurement of hardness could not be done properly. In order to eliminate this difficulty the pair of samples was grinded in such a way that the weld zone would be exposed and the indenter could reach the weld zone. To achieve this shape the material at the upper portion and side portion of the welding were removed by grinding the pair at about 45^0.

All the 16 samples were prepared and taken to measure macro-hardness. The work piece was placed on the base under the indenter as shown in Fig. 17 (a). The position of welding was controlled properly by seeing through microscope provided in the machine. The dwell time of 10 s and force of 3 kgf was set in the Vickers machine as shown in data acquisition system in Fig. 17 (b). Indentations were done on the welded portion. The diagonal of each indentation was measured by the machine and basing on formula provided in Equation 1, the hardness value was measured.

$$HV = \frac{1.8544F}{d^2}$$
(1)

Where, F = Force in kgf

d = Diameter in mm.

Fig. 17: (a) Vickers hardness machine (b) Data acquisition system

The indentations were done at three different points of welding in a welding pair and the average of hardness values were taken as final hardness value of a sample. Table 3 shows hardness values of samples.

Table 3: Weld hardness values

Run No.	HV 1	HV 2	HV 3	Avg. HV
1	265.0	262.8	263.9	263.9
2	288.9	284.0	285.4	286.1
3	281.8	283.2	283.4	282.8
4	289.0	289.1	285.9	288.0
5	281.2	284.7	284.3	283.4
6	265.6	265.8	266	265.8
7	296.4	296.8	294.5	295.9
8	280.8	286.1	286	284.3
9	288.2	287.2	288.9	288.1
10	290	293.0	287.6	290.2
11	258.1	250.1	253.8	254.0
12	258.2	254.9	260.3	257.8
13	286.1	288.2	283.7	286.0
14	278.4	275.8	274.7	276.3
15	263.0	264.4	264.3	263.9
16	248.0	248.9	247.4	248.1

3.4 HAZ MEASUREMENT

Heat affected zone (HAZ) was taken as another response parameter for optimization of process parameters. HAZ of welded portion was determined by the FESEM. But as FESEM machine incorporates very small samples and for microstructure determination smooth surface is required, so sample preparation plays an important role in determining HAZ.

In first stage the welded samples were cut by the wire EDM. It was cut in such a way that the small piece of sample would contain the weld zone. In wire EDM brass electrode was used to prepare samples of size 1 mm x 0.5 mm. All the 16 samples were cut into desired size and taken

further for polishing. The wire EDM cutting process with data acquisition system is shown in Fig. 18.

Fig. 18: (a) Cutting samples by WEDM (b) Data acquisition system

After the desired size was cut, the sample was prepared for polishing. The side portion of the welding was polished properly by means of paper polishing. The polishing side of the sample was exposed in the FESEM and microstructure was analyzed. Basing on different microstructure at the fusion zone, HAZ was calculated. Table 4 shows length of HAZ for various samples.

3.5 TAGUCHI ANALYSIS

Taguchi method of experimental design is a simple, efficient and systematic approach to optimize designs for performance and cost. It can optimize process parameters reducing fluctuation of system performance to source of variation. Unlike other methods, Taguchi method uses the target point concept and tries to put the result at target point.

3.5.1 Orthogonal array

This the important part of the Taguchi analysis. Orthogonal array means the combination of parameters which should be taken while experimenting such that the result yields same confidence as if all possible combinations will be taken. For different number of parameters and their levels Taguchi has suggested different orthogonal arrays. Here in this experiment 3 control

variables (pulse diameter, pulse frequency, scan speed) each having 4 levels were taken. So number of possible experimental runs will be 64. But according to Taguchi methodology, this experiment will be perfectly done by taking L_{16} orthogonal array. That means by taking only 16 runs we can complete the experiment with same confidence level. Orthogonal array suggested by Taguchi uses randomized order to consider all the levels of control parameters. Table 4 shows L_{16} orthogonal array design with corresponding parameter values.

Table 4: Experimental parameters and results

Run order	scan speed	pulse diameter	pulse frequency	Hardness	HAZ
1	30	0.3	1	263.9	0.05
2	30	0.6	3	286.1	0.09
3	30	0.9	5	282.8	0.14
4	30	1.2	7	288.0	0.20
5	45	0.3	3	283.4	0.06
6	45	0.6	1	265.8	0.04
7	45	0.9	7	295.9	0.13
8	45	1.2	5	284.3	0.11
9	60	0.3	5	288.1	0.06
10	60	0.6	7	290.2	0.08
11	60	0.9	1	254.0	0.04
12	60	1.2	3	257.8	0.07
13	75	0.3	7	286.0	0.06
14	75	0.6	5	276.3	0.07
15	75	0.9	3	263.9	0.09
16	75	1.2	1	248.1	0.08

CHAPTER **4**

RESULTS AND DISCUSSION

Different thickness of stainless steels were welded in lap joint configuration by using Nd:YAG laser. Influence of different process parameters such as scan speed, pulse diameter and pulse frequency on the response such as hardness and HAZ were analyzed in this section. In Taguchi methodology signal to noise ratio plays a vital role in determining influence of process parameters. As hardness to be maximized and HAZ to be minimized so accordingly signal to noise ratio was calculated by considering 'larger is better' and 'smaller is better' criteria respectively. S/N ratio was calculated by following Equation 2.

$$\eta = -10\log_{10}(MSD) \tag{2}$$

Where, η is the S/N ratio and the value of MSD (Mean Square Deviation) changes according to objective of the experiment.

For larger is better quality characteristics, $\quad MSD = (\frac{1}{y_1^2} + \frac{1}{y_2^2} + \frac{1}{y_3^2} + \cdots \frac{1}{y_N^2}) \tag{3}$

For smaller is better quality characteristics, $MSD = (y_1^2 + y_2^2 + y_3^2 + \cdots y_N^2) \tag{4}$

STATISTICA software package was used for the convenience of calculation of SN ratio and other parameters which are necessary for the determination of optimized parameters. Table 5 shows values of signal to noise ratio for each run.

Table 5: SN ratio with corresponding factor combinations

Run no.	Scan speed	Pulse diameter	Pulse frequency	Hardness	HAZ	SN Ratio hardness	SN Ratio HAZ
1	30	0.3	1	263.9	0.05	48.4288	26.0206
2	30	0.6	3	286.1	0.09	49.1304	20.9151
3	30	0.9	5	282.8	0.14	49.0296	17.0774
4	30	1.2	7	288.0	0.20	49.1878	13.9794
5	45	0.3	3	283.4	0.06	49.0480	24.4370
6	45	0.6	1	265.8	0.04	48.4911	27.9588
7	45	0.9	7	295.9	0.13	49.4229	17.7211
8	45	1.2	5	284.3	0.11	49.0755	19.1721
9	60	0.3	5	288.1	0.06	49.1909	24.4370
10	60	0.6	7	290.2	0.08	49.2539	21.9382
11	60	0.9	1	254.0	0.04	48.0967	27.9588
12	60	1.2	3	257.8	0.07	48.2257	23.0980
13	75	0.3	7	286.0	0.06	49.1273	24.4370
14	75	0.6	5	276.3	0.07	48.8276	23.0980
15	75	0.9	3	263.9	0.09	48.4288	20.9151
16	75	1.2	1	248.1	0.08	47.8925	21.9382

4.1 SINGLE OBJECTIVE OPTIMIZATION TECHNIQUE

In our project two quality characteristics such as weld hardness and HAZ were considered. First these were optimized individually by Taguchi technique. Main effect plot for SN ratio of both the parameters were drawn and a regression Equation was established between response and controllable parameters. ANOVA table for both the objectives were analyzed.

4.1.1 Taguchi methodology for Hardness

Fig. 19 shows the variation of SN ratios of hardness values with controllable parameters.
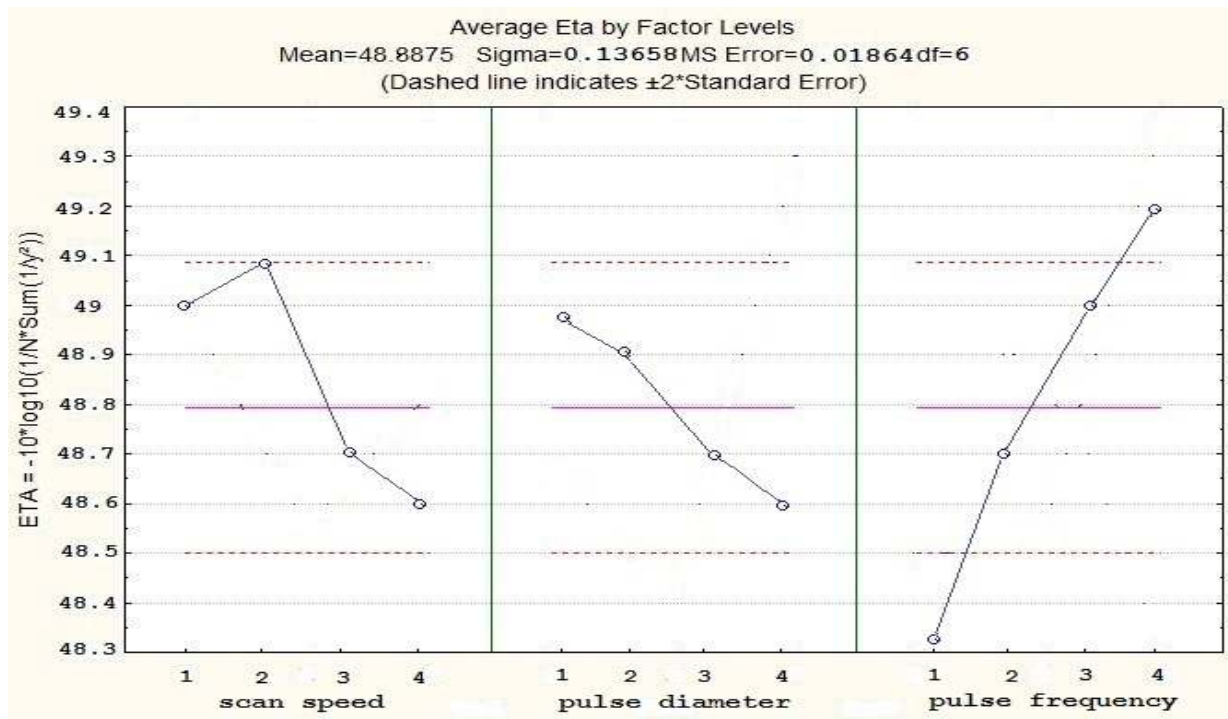
Fig. 19: Main effect plot for SN ratios of hardness

Main effect plot in Fig. 19 indicates that scan speed at 2nd level, pulse diameter at 1st level and pulse frequency at 4th level are optimized levels for maximizing weld hardness. So optimized process parameters for hardness are:

1. Scan speed: 45 mm/min
2. Pulse diameter: 0.3 mm
3. Pulse frequency: 7 Hz

50

Table 6: Analysis of Variance for SN ratios of hardness

Source	DF	Seq SS	Adj SS	Adj MS	F	P
scan speed	3	0.5184	0.5184	0.17281	9.27	0.011
pulse diameter	3	0.3313	0.3313	0.11044	5.92	0.032
pulse frequency	3	2.3617	2.3617	0.78722	42.22	0.000
Residual Error	6	0.1119	0.1119	0.01864		
Total	15	3.3233				
S = 0.1365 R-Sq = 96.6% R-Sq(adj) = 91.6%						

ANOVA for SN ratios given in Table 6 related to hardness was performed and found that all the process parameters have significant effect on hardness. Pulse frequency is the most significant factor for determining weld hardness. R^2 value of 91.6% confirms the reliability of the experiment. Later general regression analysis was performed and a relationship was established between input parameters and hardness given in Equation 5.

$$\text{Hardness} = 280 - 0.298\,(\textit{scan speed}) - 12.6\,(\textit{pulse diameter}) + 5.32\,(\textit{pulse frequency}) \quad (5)$$

4.1.2 Taguchi methodology for HAZ

Fig. 20 shows the variation of SN ratios of HAZ values with controllable parameters.
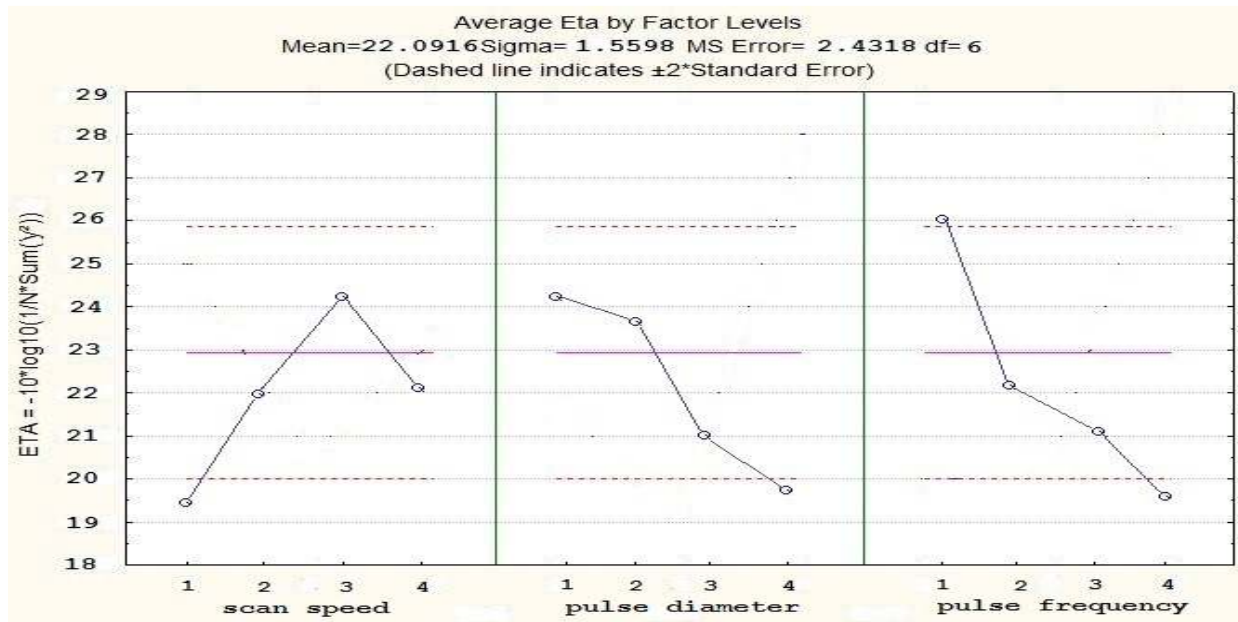
Fig. 20: Main effect plot for SN ratios of HAZ

Main effect plot in table indicates that scan speed at 3rd level, pulse diameter at 1st level and pulse frequency at 1st level are optimized levels for maximizing weld hardness. So optimized process parameters for hardness are:

1. Scan speed: 60 mm/min
2. Pulse diameter: 0.3 mm
3. Pulse frequency: 1 Hz

Table 7: Analysis of Variance for SN ratios of HAZ

Source	DF	Seq SS	Adj SS	Adj MS	F	P
scan speed	3	48.52	48.52	16.173	6.65	0.025
pulse diameter	3	68.98	68.98	22.995	9.46	0.011
pulse frequency	3	91.94	91.94	30.648	12.61	0.005
Residual Error	6	14.59	14.59	2.431		
Total	15	224.03				
S = 1.559 R-Sq = 93.5% R-Sq(adj) = 83.7%						

ANOVA for SN ratios given in Table 7 related to HAZ was performed and found that all the process parameters have significant effect on hardness. Pulse frequency is the most significant factor for determining weld hardness. R^2 value of 83.7% confirms the reliability of the experiment. Later general regression analysis was performed and a relationship was established between input parameters and hardness given in Equation 6.

HAZ = 0.047 - 0.001 (*scan speed*) + 0.067 (*pulse diameter*) + 0.01 (*pulse frequency*)   (6)

4.2 MULTI-OBJECTIVE OPTIMIZATION TECHNIQUE

As two response parameters were considered for optimization so we had to adopt one multi objective optimization techniques. In this project we had taken Grey Taguchi methodology for optimizing process parameters. In the first stage the Grey relational technique was used and then basing on the grade it was optimized by Taguchi technique.

4.2.1 Grey relational technique

Grey relational analysis is a technique to measure the correlation degree between parameters based on the similarity or difference between parameters. Grey relational methodology was used to convert two quality parameters to a single quality parameter. So that the multi objective can be converted into single objective and any optimization technique like Taguchi used for single objective can be utilized. This is done by obtaining grey relational grade from the grey relational analysis. It is characterized by less data and multi factor analysis, where these two characteristics can overcome the disadvantages of the statistical regression analysis. Grey relational grade is used as the performance characteristics in the single objective optimization technique. Then optimal laser parameters are determined using the parameter design using Taguchi technique. The step by step procedure of Grey relational analysis with result was shown below.

STEP (1): Finding out the experimental data tables through DOE as shown in Table 4.

STEP (2): Normalizing the response parameters in the domain of (0, 1) as shown in Table 8 by using Equation 7 and 8 for 'higher is better' and 'lower is better' response respectively.

$$N_{ij} = \frac{X_{ij} - (X_{ij})_{min}}{(X_{ij})_{max} - (X_{ij})_{min}} \tag{7}$$

$$N_{ij} = \frac{(X_{ij})_{max} - X_{ij}}{(X_{ij})_{max} - (X_{ij})_{min}} \tag{8}$$

Where, N_{ij}= Normalized value after grey relational generation

$(X_{ij})_{max}$= Maximum value of response parameter

$(X_{ij})_{min}$ = Minimum value of response parameter and

X_{ij}= Value of response in ith column and jth row of design matrix.

Here, i value varies from 1 to 2 and j value varies from 1 to 16.

Table 8: Grey relational generation with normalization

Run Order	Hardness	HAZ
Ideal sequence	1	1
1	0.330	0.937
2	0.795	0.687
3	0.726	0.375
4	0.835	0
5	0.738	0.875
6	0.370	1
7	1	0.437
8	0.757	0.562
9	0.836	0.875
10	0.880	0.750
11	0.123	1
12	0.203	0.812
13	0.793	0.875
14	0.590	0.812
15	0.330	0.687
16	0	0.750

STEP (3): Calculate $\Delta_{ij} = |X_{oj} - X_{ij}|$ as shown in Table 9.

Where, Δ_{ij} is the absolute value of the difference of X_{oj} and X_{ij}.

Table 9: Calculation of Δ_{ij}

Run Order	Hardness	HAZ
Ideal sequence	1	1
1	0.670	0.063
2	0.205	0.313
3	0.274	0.625
4	0.165	1
5	0.262	0.125
6	0.630	0
7	0	0.563
8	0.243	0.435
9	0.164	0.125
10	0.120	0.250
11	0.877	0
12	0.797	0.188
13	0.203	0.125
14	0.410	0.188
15	0.670	0.313
16	1	0.250

STEP (4): Calculate the grey relation co-efficient by using Equation 9. The grey relational co-efficient are presented in Table 10.

$$\gamma\,(X_{oj},X_{ij}) = \frac{\Delta_{min} + \xi\,\Delta_{max}}{\Delta_{ij} + \xi\,\Delta_{maxj}} \tag{9}$$

Where, $\gamma\,(X_{oj},X_{ij})$ = Grey relational coefficient

ξ = Distinguishing coefficient varies from 0 to 1.

Here we had taken ξ as 0.5.

Table 10: Grey relational coefficient values

Run Order	Hardness	HAZ
Ideal sequence	1	1
1	0.427	0.888
2	0.709	0.615
3	0.646	0.444
4	0.752	0.333
5	0.656	0.800
6	0.397	1
7	1	0.470
8	0.673	0.533
9	0.753	0.800
10	0.806	0.666
11	0.363	1
12	0.385	0.726
13	0.711	0.800
14	0.549	0.726
15	0.427	0.615
16	0.333	0.666

STEP (5): After determining the grey relational coefficient, we had to take average value of grey coefficients by using Equation 10. This average value is called grey relational grade. The GRG values for corresponding experiments are shown in Table 11.

$$\Gamma_n = \Sigma\,\gamma\,(X_i(k),X_j\,(k)) \tag{10}$$

Where k= Number of tests.

Table 11: Grey relational grade table

Run Order	Scan Speed	Pulse Diameter	Pulse Frequency	GRG
1	30	0.3	1	0.657
2	30	0.6	3	0.662
3	30	0.9	5	0.545
4	30	1.2	7	0.542
5	45	0.3	3	0.728
6	45	0.6	1	0.698
7	45	0.9	7	0.735
8	45	1.2	5	0.603
9	60	0.3	5	0.776
10	60	0.6	7	0.736
11	60	0.9	1	0.681
12	60	1.2	3	0.555
13	75	0.3	7	0.755
14	75	0.6	5	0.637
15	75	0.9	3	0.521
16	75	1.2	1	0.500

STEP (6): Total mean grey relational grade was calculated by using Equation 11.

$$\Gamma m = \Sigma \, \Gamma(k) \tag{11}$$

So, Γm = 1/16(0.657 + 0.662 + 0.545 + 0.542 + 0.728 + 0.698 + 0.735 + 0.603 + 0.776 + 0.736

+ 0.681 + 0.555 + 0.755 + 0.637 + 0.521 + 0.500)

= 0.6457

4.2.2 Single objective Taguchi technique

In grey relational analysis, the two objectives were converted into single objective in the form of relational grade. So grey relational grade was considered as performance characteristics and Taguchi methodology was used for optimizing controllable parameters. For determining SN ratio for grey relational grade, larger is better criteria was chosen. Equation 2 was followed for calculating S/N ratio. Here scan speed, pulse diameter, pulse frequency were chosen as input

parameters and grey relational grade was used as output parameter. Apart from SN ratio, Table 12 shows means, fits means, fits SN ratio, residual means and residual SN ratio generated by analyzing data in STATISTICA.

Table 12: DOE result of Grey based relational Taguchi method

Run Order	Scan Speed	Pulse Diameter	Pulse Frequency	Relational grade	S/N Ratio	Mean	Fits means	Fits SN	Residual means	Residual SN
1	30	0.3	1	0.657	-3.648	0.657	0.673	-3.484	-0.016	-0.164
2	30	0.6	3	0.662	-3.582	0.662	0.609	-4.290	0.052	0.707
3	30	0.9	5	0.545	-5.272	0.545	0.570	-4.872	-0.025	-0.399
4	30	1.2	7	0.542	-5.320	0.542	0.552	-5.176	-0.010	-0.143
5	45	0.3	3	0.728	-2.757	0.728	0.745	-2.512	-0.017	-0.244
6	45	0.6	1	0.698	-3.122	0.698	0.716	-2.824	-0.018	-0.298
7	45	0.9	7	0.735	-2.674	0.735	0.712	-2.981	0.022	0.307
8	45	1.2	5	0.603	-4.393	0.603	0.589	-4.629	0.013	0.235
9	60	0.3	5	0.776	-2.202	0.776	0.764	-2.271	0.011	0.068
10	60	0.6	7	0.736	-2.662	0.736	0.770	-2.158	-0.034	-0.503
11	60	0.9	1	0.681	-3.337	0.681	0.650	-3.831	0.030	0.494
12	60	1.2	3	0.555	-5.114	0.555	0.562	-5.054	-0.007	-0.059
13	75	0.3	7	0.755	-2.441	0.755	0.732	-2.781	0.022	0.340
14	75	0.6	5	0.637	-3.917	0.637	0.635	-4.012	0.001	0.094
15	75	0.9	3	0.521	-5.663	0.521	0.548	-5.260	-0.027	-0.402
16	75	1.2	1	0.500	-6.020	0.500	0.495	-5.988	0.004	-0.031

The main effects plot for S/N ratios in Fig. 21 indicates the variation of S/N ratios with respect to controllable parameters.
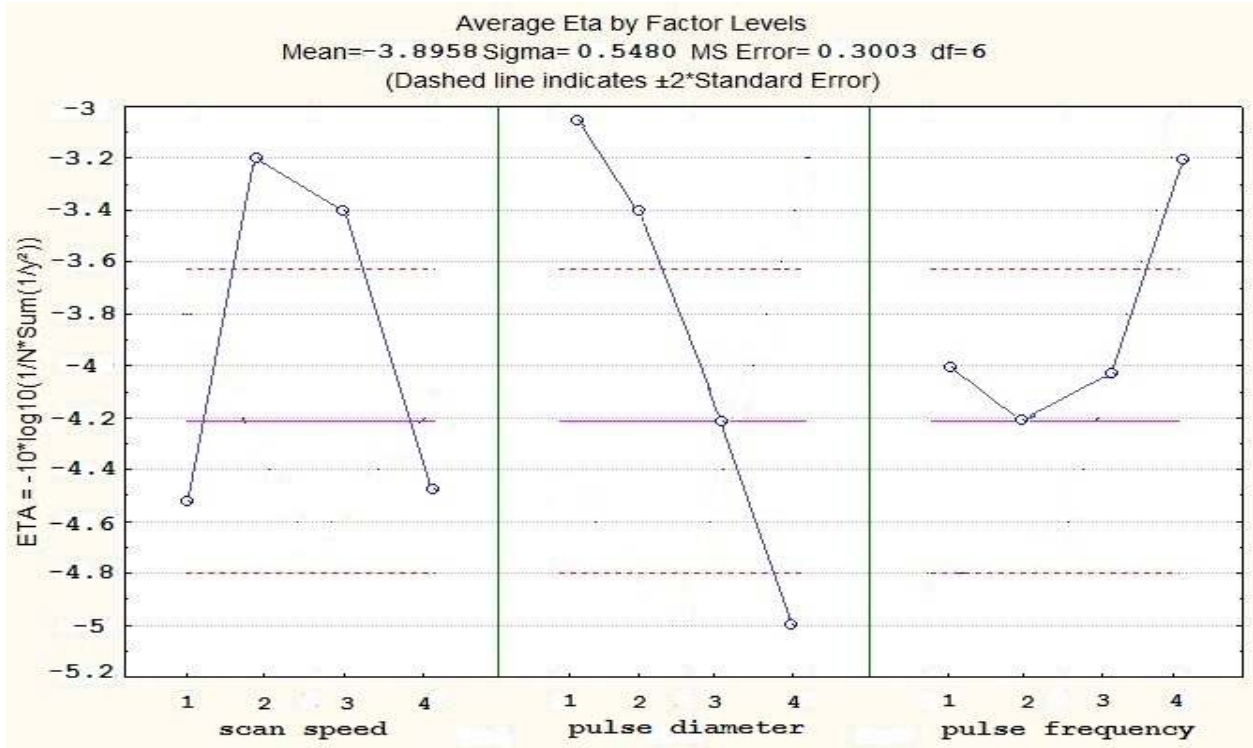
Fig. 21: Main effect plot for SN ratios of GRG

It is clear from the Fig. 21 that as pulse frequency increases SN ratio increases. This reverses in case of pulse diameter. But scan speed doesn't follow proper trend with S/N ratio. As for optimized values always maximum S/N ratio was taken so from the figure it was concluded that scan speed at 2nd level, pulse diameter at 1st level and pulse frequency at 4th level have optimized values.

ANOVA is a statistical method to estimate quantitatively the significance parameters. It is also used to determine which control factors are affecting the response in which level of action. This is done by reducing variability of control factors. If the p-value obtained from ANOVA is less than significance level (0.05), then that factor is considered to be statistically significant. The relative significance of factor can be obtained by F-ratio or percentage of contribution. The more the percentage of contribution the more significant the factor will be. So basically ANOVA is carried out to investigate the influence of the three selected control parameters. Table 13 and Table 14 show ANOVA for S/N ratio and means respectively.

Table 13: Analysis of Variance for SN ratios of GRG

Source	DF	Seq SS	Adj SS	Adj MS	F	P	% contribution
scan speed	3	5.784	5.784	1.9281	6.42	0.027	24.5
pulse diameter	3	13.850	13.850	4.6168	15.37	0.003	58.55
pulse frequency	3	2.215	2.215	0.7384	2.46	0.160	9.36
Residual Error	6	1.802	1.802	0.3003			7.61
Total	15	23.652					

Table 14: Analysis of Variance for Means of GRG

Source	DF	Seq SS	Adj SS	Adj MS	F	P
scan speed	3	0.030054	0.030054	0.010018	6.89	0.023
pulse diameter	3	0.072570	0.072570	0.024190	16.64	0.003
pulse frequency	3	0.012652	0.012652	0.004217	2.90	0.124
Residual Error	6	0.008724	0.008724	0.001454		
Total	15	0.123999				

From ANOVA of S/N ratio as shown in Table 13 it was found that p value of scan speed and pulse diameter lied below significant level which is set to be 0.05. Hence scan speed and pulse diameter are significant factors. So controlling these two parameters the quality of the weld can be regulated. The probability of pulse frequency indicates that it has least effect on quality characteristics. Hence its effect can be neglected. Same result found for effect of parameters in ANOVA of means given in Table 14.

The pulse diameter has highest percentage contribution of 58.55 followed by scan speed of 24.5% and pulse frequency of 9.36% respectively. So the pulse diameter is the most effective parameter in maximizing weld hardness and minimizing HAZ. Lower residual error validated the experiment.

The average parametric values for each level of parameters were shown in response table. Table 15 and Table 16 shows response table for signal to noise ratio and means respectively.

Table 15: Response Table for Signal to Noise Ratios of GRG

Level	scan speed	pulse diameter	pulse frequency
1	-4.456	-2.762	-4.032
2	-3.237	-3.321	-4.279
3	-3.329	-4.237	-3.946
4	-4.511	-5.212	-3.274
Delta	1.273	2.450	1.005
Rank	2	1	3

Table 16: Response Table for Means of GRG

Level	scan speed	pulse diameter	pulse frequency
1	0.6015	0.7290	0.6340
2	0.6910	0.6833	0.6165
3	0.6870	0.6205	0.6402
4	0.6032	0.5500	0.6920
Delta	0.0895	0.1790	0.0755
Rank	2	1	3

In response table Delta value indicates the variability of factors. Table 15 and Table 16 shows that pulse diameter has highest variability. Also rank of parameters in response table indicates the order at which the parameters influence the quality characteristics. So pulse diameter has greatest influence on weld hardness and HAZ.
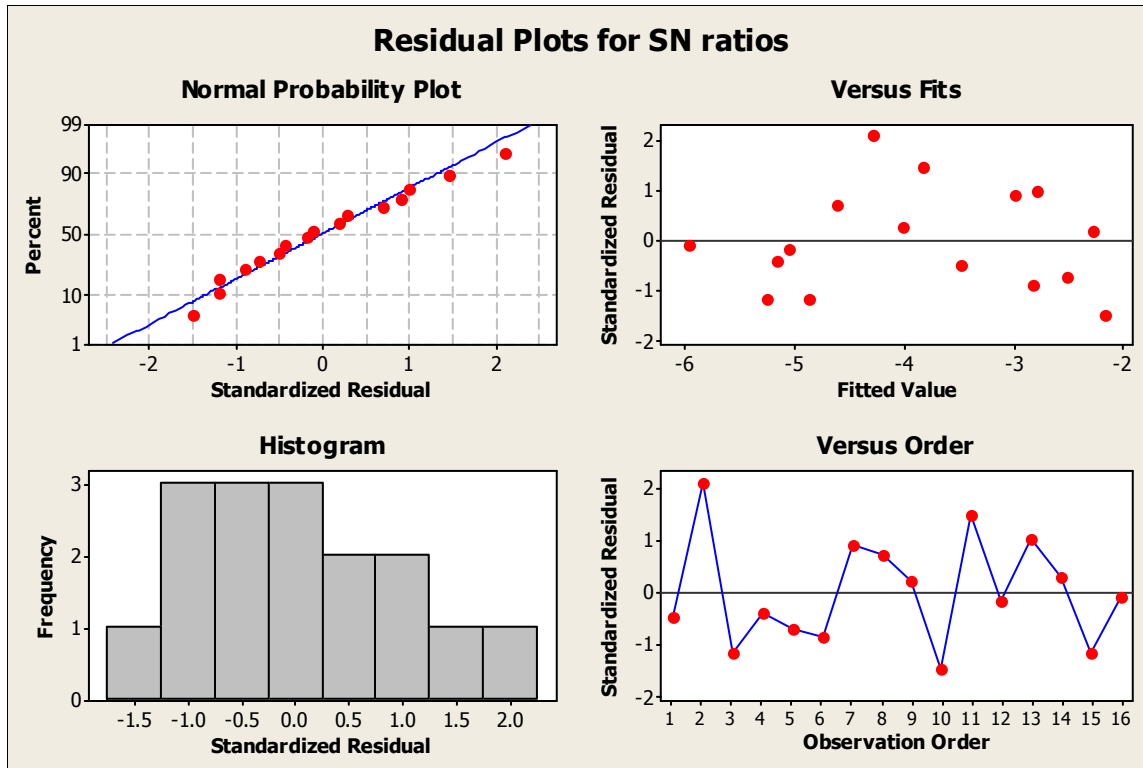
Fig. 22: Residual plots for SN ratios of GRG

From regression analysis of GRG residual plots for SN ratios were found shown in Fig. 22. It was found that the experimental data fits well to the regression line. Generally the histogram plot follows normal distribution. Here in Fig. 22 histogram plot is somehow similar to normal distribution diagram. It validates the experimental data. Verses fits and versus order follows randomized order which is desirable. The regression analysis generates a relation between GRG and process parameters given in Equation 12.

GRG = 0.756 + 0.000008 (*scan speed*) - 0.200 (*pulse diameter*)+ 0.00989 (*pulse frequency*)   (12)

4.3   PREDICTION OF TAGUCHI RESULT

The optimized Taguchi result was predicted by the software which is illustrated in Table 17. It was confirmed that scan speed at 45 mm/min, pulse diameter of 0.3 mm and pulse frequency of 7 Hz has maximum weld hardness and minimum HAZ.

Table 17: Factor levels for predictions

Scan speed (mm/min)	Pulse diameter (mm)	Pulse frequency (Hz)	S/N Ratio	Mean
45	0.3	7	-1.50767	0.820625

4.4   CONFIRMATORY TEST RESULT

The final step is to confirm the validity of the optimization technique and verify the improvement of the performance characteristics by welding same sample with predicted optimized level setting. That means again laser welding was done for the specified sample with 45 mm/min scan speed, 0.3 mm pulse diameter and 7 Hz frequency. The same procedure was followed to find weld hardness and length of heat affected zone. The weld hardness was found to be 304.77 HV and length of HAZ to be 0.0852 mm.

Again considering the predicted optimized parameters and using Equation 5 and Equation 6, weld hardness was calculated to be 300.05 HV and length of HAZ to be 0.0948.

Table 18: Comparison of result

parameters	Predicted result	Actual result	Percentage error
Weld Hardness	300.05 HV	304.77 HV	1.54%
HAZ	0.0948 mm	0.0852 mm	11.26%

Analyzing actual result we found that actual hardness number is the highest among all hardness numbers. So hardness is actually maximized in the optimized levels. But in case of length of HAZ the actual value is not the smallest among all length of heat affected zones. It is somehow elevated above the minimum length of HAZ. So length of HAZ is minimized at the optimized levels. Hence it is confirmed that the optimization technique applied is adequate and validate. Table 18 compares the predicted result and actual result of both the responses. The

percentage error in predicted result for weld hardness was calculated to be 1.54% and for length of HAZ to be 11.26%.

CHAPTER 5

CONCLUSIONS AND SUGGESTION FOR FUTURE WORK

5.1 CONCLUSIONS

Two dissimilar materials named AISI 316L stainless steel and AISI 1552 stainless steel were welded in lap joint configuration by laser welding. Taguchi methodology was used to optimize controllable variables. Some of the important salient features were observed in laser welding are discussed below.

1. Laser welding with scan speed of 45 mm/min, pulse diameter of 0.3 mm and pulse frequency of 7 Hz yields the optimal quality characteristics.
2. Hardness of weld zone was found to be 300.05 HV and length of HAZ to be 0.0948 mm at optimal setting from optimization model.
3. Hardness of weld zone was found to be 304.77 HV and length of HAZ to be 0.0852 mm experimentally at optimal setting.
4. For laser welding of austenitic stainless steel and carbon steel it was found that hardness decreases with increase in scan speed and pulse diameter whereas hardness increases with increase in pulse frequency.
5. For the same samples, HAZ decreases when scan speed increases whereas HAZ increases when pulse diameter and pulse frequency increases..
6. In the welding process pulse frequency has highest influence on determining weld hardness and length of HAZ when responses are analyzed individually. But when both the responses were considered simultaneously, it is found that pulse frequency has lowest influence on weld hardness and length of HAZ.
7. Pulse diameter is the most significant factor for determining quality characteristics when both weld hardness and length of HAZ are considered.
8. The highest SN ratio in predicted result indicates that the optimization model is adequate.
9. From predicted result of hardness and HAZ it is clear that hardness is actually maximized and HAZ is minimized approximately.

5.2 SUGGESTIONS FOR FUTURE WORK

1. Taking the same parameter at same levels as present work one model can be obtained by the help of a software. The model can be simulated with those parameters. The simulation will give rise to a simulated result. Finally, the simulated result, optimized result and experimental result should be compared.

2. The data obtained from laser welding of AISI 316L and AISI 1552 can be used in different optimization techniques and the optimization result found in each case should be compared. The best optimization technique in which desired result is obtained should be adopted.

3. The same laser welding can be done under water. The response, especially length of HAZ should be analyzed. The HAZ length can be minimized when welded under water. So the optimized result found in under water welding should be compared with present optimized welding parameters.

REFERENCES

[1]. Sun Z. AND Ion J.C. Laser welding of dissimilar metal combinations, Journal of Materials Science, 30 (1995): pp. 4205–4214

[2]. Hecht J. The history of the X-ray laser, Optics and Photonics News, 19 (2008): pp. 26–33.

[3]. Rao M.C. A brief introduction to excimer lasers: Fundamental study, International Journal of Advances in Pharmacy, 2 (2008): pp. 2277-4688

[4]. Barone M. and Selleri F. Frontiers of fundamental physics. New York, Plenum Press, 1994

[5]. http://uslugi.engineering-bp.com/pl/ciecie-laserem

[6]. Kannatey-Asibu E. Principles of laser materials processing. New Jersey, John Wiley and Sons inc., 2008

[7]. Zhang H., Tang D.Y. and Zhao L.M. Induced solutions formed by cross polarization coupling in a birefringent cavity fiber laser, Optical Society of America, 33 (2008): pp. 2317–2319

[8]. Duarte F. J. Tunable laser optics. New York, Elsevier Academic, 2003

[9]. Helbo B. Kristensen A. and Menon A. A micro-cavity fluidic dye laser, Journal of Micromechanics and Microengineering, 13 (2003): pp. 307-310

[10]. David F. A brief history of high-power semiconductor lasers, IEEE Journal of Selected Topics in Quantum Electronics, 6 (2000): pp. 6-8

[11]. Rongqing H., Alessandro D., Antonio M. and Paolo S. Injection locking in distributed feedback semiconductor lasers, IEEE Journal of Quantum Electronics, 21 (1991): pp. 6-12

[12]. http://en.wikipedia.org/wiki/Free-electron_laser

[13]. Petra T., Ultra-fast $YBa_2Cu_3O_{7-x}$ direct detectors for the THz frequency range. Karlsruhe, KIT Scientific Publishing, 2013

[14]. Rebollar E., Perez S., Hernandez J.J., Rueda D.R., Ezquerra T.A and Castillejo M. Assessment and formation mechanism of laser-induced periodic surface structures on polymer spin-coated films in real and reciprocal space, Langmuir Journal, 27 (2011): pp. 5596–5606

[15]. Kanawade R., Mahari F., Klampfl F., Rohde M., Knipfer C. and Gerk K. Qualitative tissue differentiation by analyzing the intensity ratios of atomic emission lines using laser induced breakdown spectroscopy: Prospects for a feedback mechanism for surgical laser systems, Wiley Online Publisher, 2013

[16]. http://en.wikipedia.org/wiki/Stimulated_emission

[17]. http://ethesis.nitrkl.ac.in/1856/

[18]. Lee J.Y., Ko S.H., Farson D.F. and Yoo C.D. Mechanism of keyhole formation and stability in stationary laser welding, Appl. Phys., 35 (2002): pp. 1570-1578

[19]. http://en.wikipedia.org/wiki/Nd:YAG_laser

[20]. Shields J.A., Applications of Molybdenum metals and its alloys. London, International Molybdenum Association, 2013

[21]. Thyagarajan Z. and Ghatak A.K. Fiber optic essentials, Wiley Interscience, 7 (2007): pp. 34-38

[22]. http://www.mar.ist.utl.pt/jgordo/Artigos/novos%20processos%20tecnol%C3%B3gicos%20update%20_2_.pdf

[23]. Tsai F. and Asibu E.K. Modeling of conduction mode laser welding process for feedback control, Journal Of Manufacturing Science And Engineering, 122 (2000): pp. 420-428

[24]. https://www.google.co.in/conductionmodewelding

[25]. https://www.google.co.in/keyholemodewelding

[26]. Avetissian H.K., Ghazaryan A.G. And Mkrtchian G.F. Relativistic theory of inverse-bremsstrahlung absorption of ultrastrong laser radiation in plasma, Journal of Physics, 46 (2013): pp. 1088-1096

[27]. Jin X., Cheng Y., Zeng L., Zou Y. and Zhang H. Multiple reflections and fresnel absorption of gaussian laser beam in an actual 3D keyhole during deep-penetration laser welding, International Journal of Optics, 2012 (2012): pp. 288-295

[28]. Na X, Zhang Y, Liu Y and Walcott B. Nonlinear identification of laser welding process, IEEE Transactions on Control Systems Technology, 18 (2010): pp. 927-934.

[29]. Seang C., David A.K. and Ragneau E. Effect of Nd:YAG laser welding parameters on the hardness of lap joint: experimental and numerical approach, Phys Procedia, 41 (2013): pp. 38-40

[30]. Wang G., Wu A., Zou G., Zhao Y., Chen Q. and Ren J. Bending properties and fracture behavior of Ti-23Al-17Nb alloy laser beam welding joints, Tsinghua Sci Technol., 14 (2009): pp. 293-299.

[31]. Sun A., Liu J. and Liu W. The laser beam welding of ferritic stainless steel for the motor vehicle exhaust 409L, Proc 2011 Int. Conf. Electron Mech. Eng. Inf. Technology, 8 (2011): pp. 3931-3933.

[32]. Shenghai Z., Yifu S. and Huijuan Q. The technology and welding joint properties of hybrid laser-TIG welding on thick plate, Optics and Laser Technology, 48 (2013): pp. 381-388

[33]. Khan M.M.A., Romoli L. and Dini G. Laser beam welding of dissimilar ferritic/martensitic stainless steels in a butt joint configuration, Optics and Laser Technology, 49 (2013): pp. 125-136

[34]. Sokolov M., Salminen A., Kuznetsov M. and Tsibulskiy I. Laser welding and weld hardness analysis of thick section S355 structural steel, Mater Des, 32 (2011): pp. 5127-5131

[35]. Khan M.M.A., Romoli L., Fiaschi M., Dini G. and Sarri F. Experimental design approach to the process parameter optimization for laser welding of martensitic stainless steels in a constrained overlap configuration. Optics and Laser Technology, 43 (2011): pp. 158-172

[36]. Klimpel A. and Lisiecki A. Laser welding of butt joints of austenitic stainless steel AISI 321, Journal of Achievements in Materials and Manufacturing Engineering, 25 (2007) pp. 256-267

[37]. Sathiya P., Panneerselvam K. and Soundararajan R. Optimal design for laser beam butt welding process parameter using artificial neural networks and genetic algorithm for super austenitic stainless steel, Optics and Laser Technology, 44 (2012): pp. 1905-1914

[38]. Fortunato A., Ascari A., Orazi L., Cuccolini G., Campana G. and Tani G. Numerical simulation of nanosecond pulsed laser welding of eutectoid steel components, Optics and Laser Technology, 44 (2012): pp. 1999-2003

[39]. Pan L.K., Wang C.C., Hsiao Y.C. and Ho K.C. Optimization of Nd:YAG laser welding onto magnesium alloy via Taguchi analysis. Optics and Laser Technology, 37 (2005): pp. 33-42

[40]. Acherjee B., Kuar A. S., Mitra S. and Misra D. Modeling and analysis of simultaneous laser transmission welding of polycarbonates using an FEM and RSM combined approach, Optics and Laser Technology, 44 (2012): pp. 995–1006

[41]. Padmanaban G. and Balasubramanian V. Optimization of laser beam welding process parameters to attain maximum tensile strength in AZ31B magnesium alloy, Optics and Laser Technology, 42 (2010): pp. 1253–1260

[42]. Pan L.K., Wang C.C., Wei S.L. and Sher H.F. Optimizing multiple quality characteristics via Taguchi method-based grey analysis, Journal of Materials Processing Technology, 182 (2007): pp. 107–116

[43]. Muhammad N., Manurung Y. H. P., Hafidzi M., Abas S. K., Tham G. and Haruman E. Optimization and modeling of spot welding parameters with simultaneous multiple response consideration using multi-objective Taguchi method and RSM, Journal of Mechanical Science and Technology, 26 (2012): pp. 2365–2370